

2017

# Surface-enhanced Raman spectroscopy (SERS) for the qualitative analysis of synthetic piperazines

---

<https://hdl.handle.net/2144/26942>

*"Downloaded from OpenBU. Boston University's institutional repository."*

BOSTON UNIVERSITY  
SCHOOL OF MEDICINE

Thesis

**SURFACE-ENHANCED RAMAN SPECTROSCOPY (SERS) FOR THE  
QUALITATIVE ANALYSIS OF SYNTHETIC PIPERAZINES**

by

**JESSAMYN ROSE WARD**

B.S., Central Connecticut State University, 2014

Submitted in partial fulfillment of the  
requirements for the degree of  
Master of Science

2017

© 2017 by  
JESSAMYN ROSE WARD  
All rights reserved

Approved by

First Reader

---

Sabra Botch-Jones, M.S., M.S., M.A., D-ABFT-FT  
Assistant Professor, Program in Biomedical Forensic Sciences  
Department of Anatomy & Neurobiology

Second Reader

---

Lawrence D. Ziegler, Ph.D.  
Professor, Department Chair  
Department of Chemistry

Third Reader

---

Amy N. Brodeur, M.F.S., F-ABC  
Assistant Professor, Program in Biomedical Forensic Sciences  
Department of Anatomy & Neurobiology

## ACKNOWLEDGMENTS

First and foremost, I would like to thank my thesis advisor, Assistant Professor Sabra Botch-Jones, for her support and mentorship throughout the past two years. I have learned so much from Professor Botch-Jones in the classroom, in the laboratory, and in how to handle the demanding field of forensic science. Without her, this project, nor my academic career at Boston University, would have been nearly as successful.

I would also like to thank the members of the Ziegler Research group of the Boston University Department of Chemistry, especially Dr. Ranjith Premasari, Ms. Ying Chen and Mr. Harrison Ingraham, for their countless hours spent helping me become a more efficient and knowledgeable scientist in the field of SERS. Even though everyone had their own projects, Dr. Premasari, Ms. Chen and Mr. Harrison were always willing to meet with me to discuss this project. I thank Dr. Larry Ziegler, principle investigator, for always pushing me to achieve greater in my research. The work ethic and professionalism I witnessed and absorbed in the Ziegler laboratory is something I will carry with me in my future professional endeavors.

Lastly, I would like to thank my parents, sister and fiancé for their support during the whirlwind of graduate school. I have grown as an individual both personally and professionally over the last two years and am greatly looking forward to my career as a forensic scientist for years to come.

**SURFACE-ENHANCED RAMAN SPECTROSCOPY (SERS) FOR THE  
QUALITATIVE ANALYSIS OF SYNTHETIC PIPERAZINES**

**JESSAMYN ROSE WARD**

**ABSTRACT**

Designer drugs are some of the most commonly abused substances in the world (1). They are synthesized through slight chemical modifications of existing substances, evading the law while maintaining the desired effects of the pharmaceutical or illicit substance. These drugs are often marketed as “herbal” or “natural,” but are fully synthetic. Due to their constant, rapid emergence, there is a need for a rapid method of identification, both in the field as well as in the laboratory (1, 2).

One group of these designer drugs are synthetic piperazines. Named for the piperazine ring found in their chemical structures, synthetic piperazines are central nervous system stimulants that have the reputation of mimicking the psychoactive effects of the illicit compounds amphetamine and 3, 4-methylenedioxymethamphetamine (MDMA) (3). Over the past 10 years, synthetic piperazine cases submitted to forensic laboratories in the United States have greatly increased, including a 30-fold increase between 2007 and 2009 alone (4).

Surface enhanced Raman spectroscopy (SERS) was investigated as a method for the rapid qualitative analysis of synthetic piperazines. SERS is a type of vibrational spectroscopy, which utilizes the interaction of light and matter to elucidate details of the

chemical structure of a molecule. SERS combines laser spectroscopy with the optical properties of metallic nanostructures, resulting in strongly enhanced signals from the Raman scattering of light. Each chemical structure will give a unique SERS spectrum and this, coupled with the minimal-to-no sample preparation and the portability of a SERS instrument, makes SERS a strong candidate for the identification of not only synthetic piperazines, but all designer drugs.

To evaluate the use of SERS for the qualitative analysis of synthetic piperazines, eight synthetic piperazines were adsorbed onto a SERS substrate. The interaction with the gold nanoparticles enhanced the Raman scattering for all eight of the synthetic piperazines and SERS spectra were obtained. All eight drugs were found to give a robust and reproducible signal, requiring a fewer number of scans, less laser power, and less time for analysis compared with traditional Raman spectroscopy. When compared with traditional Raman spectra, the synthetic piperazines demonstrated sensitivity enhancement factors of up to  $10^8$  using SERS.

A partial least squares-discriminant analysis (PLS-DA) statistical model was built and used to evaluate the analytical sensitivity and specificity of the SERS method. The PLS-DA model helped determine a limit of detection of 10  $\mu\text{g/mL}$  of BZP. All eight synthetic piperazines could be identified by the statistical model below an error rate of 20% when compared to each other- a strong indication of a method with high specificity.

Through this research, it has been demonstrated that SERS can be applied efficiently as a qualitative technique for the analysis of synthetic piperazines.

## TABLE OF CONTENTS

Title Page .....	i
Copyright Page .....	ii
Reader's Approval Page .....	iii
Acknowledgments .....	iv
Abstract .....	v
TABLE OF CONTENTS.....	vii
LIST OF TABLES .....	x
LIST OF FIGURES .....	xi
LIST OF EQUATIONS .....	xiii
LIST OF ABBREVIATIONS.....	xiv
1. INTRODUCTION .....	1
1.1 Synthetic Piperazines.....	1
1.1.1 Synthetic Piperazines .....	1
1.1.2 Current Methods for the Qualitative Analysis of Synthetic Piperazines .....	4
1.2 Raman Spectroscopy and Surface Enhanced Raman Spectroscopy .....	7
1.2.1 Raman Spectroscopy .....	7
1.2.2 Surface-Enhanced Raman Spectroscopy.....	10
1.2.3 Current Uses of Raman Spectroscopy and SERS in Forensic Drug Chemistry	12
1.3 Density Functional Theory .....	14
1.4 Partial Least Squares- Discriminant Analysis with Barcode.....	17
2. MATERIALS AND METHODS.....	20

2.1 Synthetic Piperazines.....	20
2.2 Spectral Acquisition .....	21
2.2.1 SERS Spectral Acquisition .....	21
2.2.2 Raman Spectral Acquisition.....	22
2.2.3 DFT Calculations and Theoretical Raman Spectral Acquisition .....	24
2.3 Statistical Analysis .....	25
2.3.1 Enhancement Factors .....	25
2.3.2 PLS-DA Model .....	26
2.3.3 Sensitivity.....	26
2.3.4 Specificity .....	27
3. RESULTS AND DISCUSSION.....	29
3.1 SERS.....	29
3.1.1 SERS Spectra .....	29
3.1.2 SERS versus Raman of Synthetic Piperazines in Solution.....	31
3.1.3 Raman of Synthetic Piperazines in Power Form.....	35
3.2 DFT Calculations and Band Assignments.....	36
3.3 Statistical Analysis .....	42
3.3.1 Enhancement Factors .....	42
3.3.2 PLS-DA Model .....	43
3.2.3 Sensitivity.....	44
3.2.4 Specificity .....	46
4. CONCLUSIONS .....	48

4.1 Future Direction.....	48
4.2 Evaluation of the Method .....	49
APPENDIX A:.....	52
LIST OF JOURNAL ABBREVIATIONS .....	61
BIBLIOGRAPHY .....	62
CURRICULUM VITAE.....	67

## LIST OF TABLES

Table 1. Method differences between SERS and Raman of solutions .....	34
Table 2. Band assignments for BZP. ....	39
Table 3. Band assignments for DCPD.....	41
Table 4. Enhancement factors of synthetic piperazines.....	42
Table 5. Error rates from BZP dilutions. ....	46
Table 6. Error rates from the blind test.....	47
Table 8. Band Assignments for FBZP.....	58
Table 9. Band assignments for mCPD.....	58
Table 10. Band Assignments for MBZP.....	59
Table 11. Band Assignments for MeOPD.....	59
Table 12. Band Assignments for pFPP.....	60
Table 13. Band Assignments for TFMPP.....	60

## LIST OF FIGURES

Figure 1. Chemical structure of synthetic piperazines (5) .....	2
Figure 2. The wave nature of light. (Created by author) .....	7
Figure 3. Schematic representation signals from Rayleigh and Raman scattering .....	9
Figure 4. The path of light in SERS.....	12
Figure 5. Results from an optimization calculation of BZP. ....	15
Figure 6. Result from the frequency calculation of BZP.....	16
Figure 7. Visual representative of the Barcode used in PLS-DA with the synthetic piperazines.....	19
Figure 8. SERS Substrates. ....	22
Figure 9. SERS spectra of eight synthetic piperazines .....	29
Figure 10. SERS spectrum of BZP. ....	30
Figure 11. SERS and Raman spectra of pFPP. ....	33
Figure 12. Lowest energy geometry of BZP. The benzene ring is planar and the piperazine ring is in a chair conformation. This was mostly consistent with each synthetic piperazine.....	36
Figure 13. Comparison of BZP spectra from SERS and DFT calculations.....	37
Figure 14. The letter designations used for the parts of the molecules. A is the piperazine ring and any of its constituents. B is the group of molecules that connect the piperazine ring to the benzene ring. C is the benzene ring and any of its constituents. ....	38
Figure 15. All DCPD spectra.....	40

Figure 16. The DCPD vibrational mode at 1082 cm <sup>-1</sup> .....	41
Figure 17. PLS-DA prediction value plots. ....	43
Figure 18. SERS spectra from BZP dilutions.....	45
Figure 19. All mCPP spectra. ....	49
Figure 20. SERS Spectrum of DCPD.....	52
Figure 21. SERS Spectrum of FBZP.....	52
Figure 22. SERS Spectrum of MBZP.....	53
Figure 23. SERS Spectrum of mCPP.....	53
Figure 24. SERS Spectrum of MeOPP.....	54
Figure 25. SERS Spectrum of pFPP.....	54
Figure 26. SERS Spectrum of TFMPP.....	55
Figure 27. All MBZP spectra.....	55
Figure 28. All FBZP spectra.....	56
Figure 29. All MeOPP spectra.....	56
Figure 30. All pFPP spectra.....	57
Figure 31. All TFMPP spectra.....	57

## LIST OF EQUATIONS

Equation 1. The speed of light. ....	7
Equation 2. Energy of a photon. ....	8
Equation 3. Electron density function. ....	15
Equation 4. Energy functional .....	15
Equation 5. Calculation of a cross section. ....	25
Equation 6. Calculation of an enhancement factor.....	25

## LIST OF ABBREVIATIONS

BZP	1-Benzylpiperazine
<i>c</i>	Speed of light
cm <sup>-1</sup>	Wavenumbers
DCPP	2,3-Dichlorophenylpiperazine
DFT	Density functional theory
<i>E</i>	Energy
EF	Enhancement factor
EMCDDA	European Monitoring Center for Drugs and Drug Addiction
EMIT	Enzyme-multiple immunoassay
FBZP	1-(4-Fluorobenzyl)-piperazine
FPIA	Fluorescence polarization immunoassay
GC	Gas chromatography
HCl	Hydrochloride (salt form)
HPLC-DAD	High pressure liquid chromatography- diode array detection
Hz	Hertz
IR	Infrared
LLE	Liquid/liquid extraction
LOD	Limit of detection
MBZP	4-Methyl-1-benzylpiperazine
mCPP	1-(3-Chlorophenyl)-piperazine

MDMA	3,4-Methylenedioxyamphetamine
MeOPP	1-(4-Methoxyphenyl)-piperazine
MS	Mass spectrometry
NA	Numerical aperture
NFLIS	National Forensic Laboratory Information System
NPD	Nitrogen-phosphorous detector
$h$	Planck's constant
pFPP	1-( <i>Para</i> -fluorophenyl)-piperazine
PLS-DA	Partial least squares- discriminant analysis
SERS	Surface-Enhanced Raman Spectroscopy
SiO <sub>2</sub>	Silicon dioxide
SPE	Solid-phase extraction
SWGDRUG	Scientific Working Group for the Analysis of Seized Drugs
SWGTOX	Scientific Working Group for Forensic Toxicology
TFMPP	1-(3-Trifluoromethylphenyl)-piperazine
$\nu$	Frequency
$\lambda$	Wavelength
WiRE	Windows Based Raman Environment (software)

## **1. INTRODUCTION**

### **1.1 Synthetic Piperazines**

#### *1.1.1 Synthetic Piperazines*

Synthetic, or designer drugs, are some of the most commonly abused substances in the world (1). Designer drugs are also referred to as novel psychoactive substances, which are synthesized through chemical modifications of illicit or pharmaceutical drugs that maintain desired effects but evade the law. These goals are achieved by altering the molecular structure slightly from illicit or pharmaceutical form. Often, consumers of designer drugs are young people in dance clubs, rave scenes, or music festivals, as psychoactive substances are believed to enhance these experiences. These compounds are most commonly purchased on the internet, where they are marketed as “legal highs” (1).

Among these designer drugs is a class of compounds known as synthetic piperazines. Named for the piperazine ring found in their chemical structures (Figure 1), synthetic piperazines are central nervous system stimulants that have the reputation of mimicking the psychoactive effects of the illicit compounds amphetamine and 3,4-methylenedioxymethamphetamine (MDMA) by binding to serotonin receptors in the brain (3). These drugs are synthesized through the chemical modification of the pharmaceutical drug piperazine, which was originally marketed as an anthelmintic (4). Although synthetic piperazines are often marketed as “herbal” or “natural,” they are fully synthetic and are classified as derivatives of either 1-benzylpiperazine (BZP) or 1-phenylpiperazine (2).

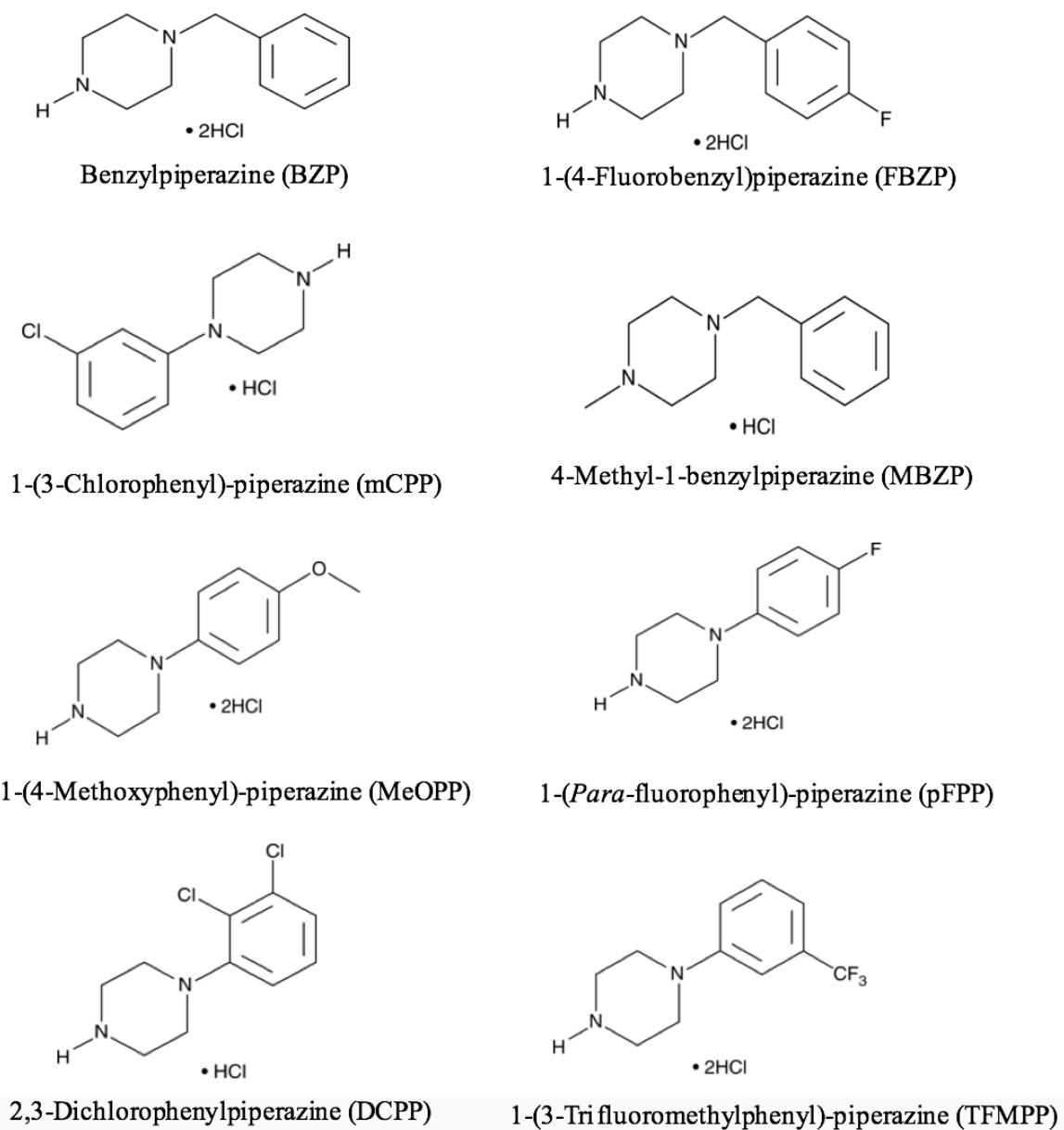


**Figure 1. Chemical structure of synthetic piperazines (5)**

BZP has been available on the internet since early 2000 where it has been sold as capsules, tablets and free powder under the name “A2” as the hydrochloride (HCl) form (3). It has also been sold under the names “Frenzy” and “Nemesis.” Consumption of

synthetic piperazines is often through oral administration or insufflation, although injection or smoking is possible (2). Although BZP was permanently scheduled in March of 2004 as a Schedule I compound by the U.S. Department of Justice Drug Enforcement Administration, its use has increased over time; by 2008, BZP appeared on the list of top 25 drugs reported to the National Forensic Laboratory Information System (NFLIS) (6). The number of BZP cases submitted to U.S. forensic laboratories grew from 437 in 2007 to 13,822 in 2009 (4). By 2010, 44 states reported synthetic piperazine cases to NFLIS, most being either BZP or 1-(3-trifluoromethylphenyl)-piperazine (TFMPP) (7).

The U.S. is not the only country that has seen abuse of synthetic piperazines (8). BZP was first sold on an European internet website in 2000 (3). While the United States has mostly seen BZP and TFMPP in forensic casework, Europe has seen higher rates in the abuse of 1-(3-chlorophenyl)piperazine (mCPP). By 2006, the European Monitoring Center for Drugs and Drug Addiction (EMCDDA) estimated that 10% of illicit tablets sold in the European Union contained mCPP (8). In that year, 22 Member States of the European Union reported mCPP seizures to the EMCDDA, ranging from a six-tablet seizure in Luxembourg to approximately 145,000 tablets seized in one German case (8). Widespread abuse of synthetic piperazines has also been reported in New Zealand and Australia (9).

As novel psychoactive substances, synthetic piperazines share common effects with stimulants such as amphetamine and MDMA, although BZP exhibits one-tenth the potency of amphetamine (4). These effects include euphoria, mood elevation, increased sociability and skin tingling. Higher doses of synthetic piperazines can have

hallucinogenic effects not present in lower doses. It is reported that MDMA-like effects are achieved by mixing BZP and TFMPP, and thus, these two compounds are often found combined in tablet form (4). Deaths have been reported with the use of BZP and TFMPP; however, most deaths were not the direct result of BZP or TFMPP toxicity, but by a loss in motor control, resulting in a fatal fall or traffic accident (10).

In a study out of New Zealand, where BZP was unrestricted at the time, it was shown that BZP toxicity shows a wide array of adverse effects (9). Between April and September of 2005, 61 patients who presented in the Emergency Department on 80 occasions had taken an average of 4.5 BZP tablets. The patients ranged in age from 15 to 36 years old. Mild to moderate toxicity presented itself with symptoms such as insomnia, agitation, anxiety, nausea, vomiting, palpitations, dystonia and urinary retention. Some adverse effects lasted up to 24 hours. Severe and life-threatening toxicity was also observed. Fifteen patients experienced seizures and two patients had severe respiratory and metabolic acidosis. The authors concluded that BZP can cause severe and unpredictable toxicity and is also dangerous due to its narrow safety margin in dosing (9).

### *1.1.2 Current Methods for the Qualitative Analysis of Synthetic Piperazines*

Multiple difficulties arise with the analysis of novel psychoactive substances in forensic casework (11). First, there is difficulty obtaining information about current trends in drugs of abuse, as these trends are constantly changing. In order to have up-to-date information, it is necessary to regularly check the internet for online suppliers and drug user forums for emerging trends. Second, the speed at which novel psychoactive

substances appear on the drug market leads to a lack of certified reference material needed for method development and validation. This, and the alarming rate at which novel psychoactive substances emerge, causes difficulty in developing methods of detection as fast as drugs are released on the market and abused by users. Many novel psychoactive substances are either not detected by the standard immunoassay reagents used for drug screening or generate misleading results. This is due to the similarities in chemical structure and common pharmacodynamics in the body between novel psychoactive substances and illicit drugs. For these reasons, clinical and forensic drug testing laboratories have turned to more laborious methods, such as mass spectroscopy, for detection of novel psychoactive substances (11).

Soon after synthetic piperazines were observed in forensic casework, there was a push for method development and validation (3). The earliest methods developed for the detection of synthetic piperazines involved labor-intensive liquid/liquid extractions (LLE) of synthetic piperazine powder, specifically from BZP capsules, using multiple reagents such as potassium hydroxide, sodium sulfate, and *tert*-butyl methyl ether. The use of immunoassays designed to detect amphetamine-like substances was evaluated first because BZP is believed to act on the same receptors in the brain as amphetamine (3). Two different amphetamine-like immunoassays were used: a fluorescence polarization immunoassay (FPIA) and an enzyme-multiplied immunoassay technique (EMIT). At a concentration of 100 µg/mL, BZP was not detected using FPIA technology, but did cross-react when using EMIT. Gas chromatography (GC) with a nitrogen phosphorous detector (NPD) or a mass spectrometer (MS) were also evaluated. With both GC-NPD and GC-

MS, BZP and TFMPP were unambiguously identifiable, both with and without derivatization (3). More recently, a high-pressure liquid chromatography with diode array detection (HPLC-DAD) method was developed and used to create a library of novel psychoactive substances data for forensic use. Among the different novel psychoactive substances detected, BZP, mCPP and 1-(4-methoxyphenyl)-piperazine (MeOPP) were recorded (12).

Although many of the methods mentioned, including GC-NPD, GC-MS and HPLC-DAD, can unambiguously identify different synthetic piperazines, these methods are labor-intensive, require multiple chemical reagents, and do not give rapid results. These methods would be adequate for use in a toxicology laboratory or in a drug chemistry laboratory after drugs have been seized. However, these methods could not be used in the field for rapid detection or be carried out by non-scientists. There is a critical need to rapidly identify novel psychoactive substances, including synthetic piperazines, in the field for multiples reasons. First, the number of drug-related Emergency Department visits in the United States doubled between 2004 and 2009 (13). A rapid, specific test that could be used by medical personnel would be critical for identifying the drugs a patient ingested so that the appropriate medical treatment could be administered. Another use for a rapid, easy-to-use method is for law enforcement. A portable method that could be kept in a law enforcement vehicle could help identify a driver under the influence of drugs, much like a breath analyzer, using the driver's saliva. A non-invasive method is necessary for collection on the side of the road or other public locations. Law enforcement officials could also use a portable method for the identification of illicit

substances in different physical forms at the scene to determine if a drug arrest is warranted.

## 1.2 Raman Spectroscopy and Surface Enhanced Raman Spectroscopy

### 1.2.1 Raman Spectroscopy

Electromagnetic radiation, also known as light, can be physically described as both a wave and a particle (14). As a wave, light is characterized by either its wavelength,  $\lambda$ , or its frequency,  $\nu$ . Together, these characteristics are used to determine the speed of light,  $c$ , which in Equation 1 is the speed of light in a vacuum, when light is at its fastest. When light enters any media, such as air or water, it travels slower than in a vacuum. (14). Light, as a wave, has oscillating electric and perpendicular polarized magnetic fields, which are both perpendicular to the direction of travel of the wave of light (Figure 2).

Equation 1. The speed of light.  $c = \lambda\nu$

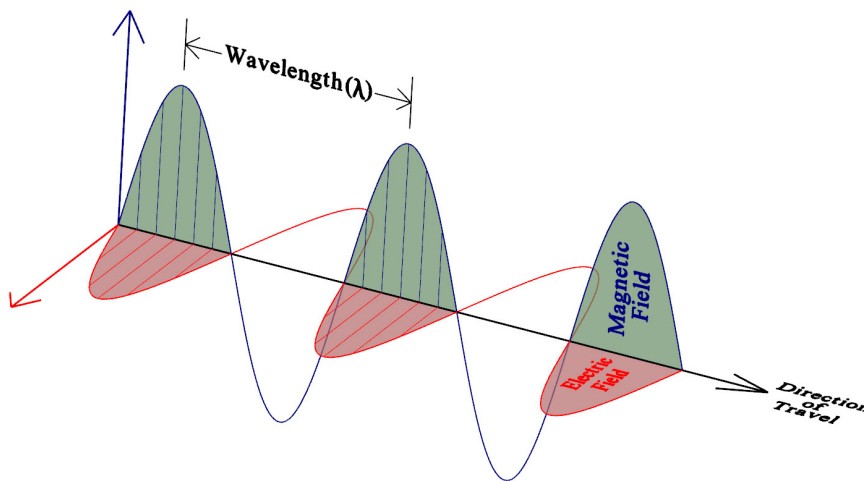


Figure 2. The wave nature of light.

Light also behaves as a particle, which individually are called photons (14). The energy ( $E$ ) of a single photon is proportional to the frequency of the wave and is described in Equation 2 using Planck's constant,  $h$ . Equation 2 recognizes both the particle and wave nature of electromagnetic radiation. These physical characteristics of light are important to understand when discussing the theory behind many types of chemical instrumentation, including vibrational spectroscopy (14).

**Equation 2. Energy of a photon.**  $E = h\nu$

Vibrational spectroscopy is a field of science which studies interactions between electromagnetic radiation and the molecular motions of matter (15). The goal of these studies is often to elucidate details of the chemical structure of the matter. Vibrational spectroscopy is often utilized because it is easily performed, reproducible, and the results can be both qualitative and quantitative. Two common types of vibrational spectroscopy include Infrared (IR) spectroscopy and Raman spectroscopy (15).

When a sample is irradiated with an electromagnetic light beam, this incident light can be transmitted, absorbed, or scattered through its interaction with the matter. IR spectroscopy measures the transmitted or absorbed light, whereas Raman spectroscopy analyzes the scattered light (16). Light can scatter in two different ways. Rayleigh, or elastic scattering, is light that scatters from the sample with the same frequency as the incident light. Photons that undergo Rayleigh scattering produce stronger signals than Raman because the vast majority of photons scatter elastically. Raman, or inelastic scattering, is light that scatters with a frequency higher or lower than the incident light. In Raman scattering, a change in the wavelength of the scattered radiation is observed

caused by the excitation or relaxation of molecular vibrational levels (17). Raman scattering produces a weaker signal than Rayleigh scattering because only a small portion of the photons (approximately  $10^{-5}\%$ ) from the incident light undergo Raman scattering (Figure 3) (18). In Raman spectroscopy, the vibrational frequency is measured as a shift from the incident light frequency, also known as the Raman shift. Each peak in a Raman spectrum is also called a band (16).

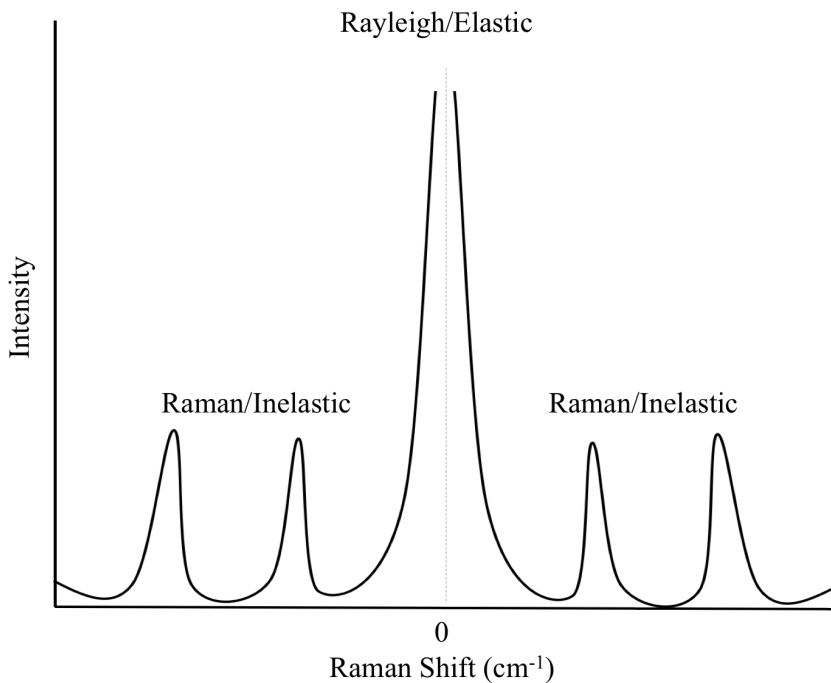


**Figure 3. Schematic representation of signals from Rayleigh and Raman scattering\*.**

Raman spectroscopy utilizes the ultraviolet-visible-near IR range of the electromagnetic radiation spectrum, which has frequencies in the  $10^{14}$ - $10^{16}$  hertz (Hz, units of cycles per second) range. For this reason, it is easier to describe the frequency in

\* For Figure 3, the top of the peak due to Rayleigh scattering is not shown because, in reality, this band would be too tall in relation to the Raman band to be depicted accurately in this schematic.

terms of wavenumbers, which is the reciprocal of the wavelength ( $1/\lambda$ ) and has units of centimeters<sup>-1</sup> ( $\text{cm}^{-1}$ ) (14). It is also preferable to use wavenumbers for describing vibrational spectra because these units, in contrast to wavelength, are directly proportional to energy.

### *1.2.2 Surface-Enhanced Raman Spectroscopy*

Surface-enhanced Raman spectroscopy (SERS) is a vibrational spectroscopic technique that combines laser spectroscopy with the optical properties of metallic nanostructures<sup>1</sup>, resulting in strongly increased Raman scattering signals (19). In 1977, Jeanmaire and Van Duyne first demonstrated that Raman scattering intensity can be greatly enhanced when the sample of interest is adsorbed on the surface of a nanostructured metal substrate (20). This surface enhancement effect, hence name SERS, results when the incident and scattered radiation is resonant with localized surface plasmon resonances (SPR) of the nanostructured surface. Hence, the laser light must be matched to the SPR of the SERS active substrate. When a molecule is in close proximity ( $< 5$  nm) of the metal nanostructured surface, some of its Raman active vibrational modes are greatly enhanced in the Raman spectrum due to this SPR resonance, which effectively generates larger electromagnetic fields at the incident and scattered frequencies and, therefore, a greatly amplified signal is produced (17). In addition to this electromagnetic enhancement mechanism, there is also a weaker chemical enhancement mechanism that generally contributes to observed SERS intensities. The chemical enhancement occurs when there is a new charge-transfer state produced between the metal substrate and the

adsorbed molecule. This enhancement is specific to the site where the molecule adsorbs to the substrate. Raman scattering is more strongly enhanced for molecules closer to the metal substrate and for vibration modes that have polarization components perpendicular to the surface (17, 21). This orientation effect and chemical enhancement mechanism can lead to SERS spectra that have different relative intensities than normal Raman spectra.

To obtain a SERS spectrum, the sample is loaded on the SERS substrate, which is generally made of silver or gold nanoparticles, and is placed under the microscope (16). A laser beam, which is the incident light, is passed through the objective lens of the microscope and focused onto the sample. At the sample, that light is either absorbed, transmitted, or scattered. The elastic, or Rayleigh, scattered light is filtered out by a high optical density notch filter, but the collected backscattered inelastic, or Raman light, is reflected by a series of mirrors to a monochromator where the dispersed light is read by a charge-coupled device detector (CCD). After the CCD, the electrical signal is amplified and converted into a spectrum by software on a computer. The resulting spectrum is plotted as the Raman shift in wavenumbers versus the signal intensity (Figure 4) (16).

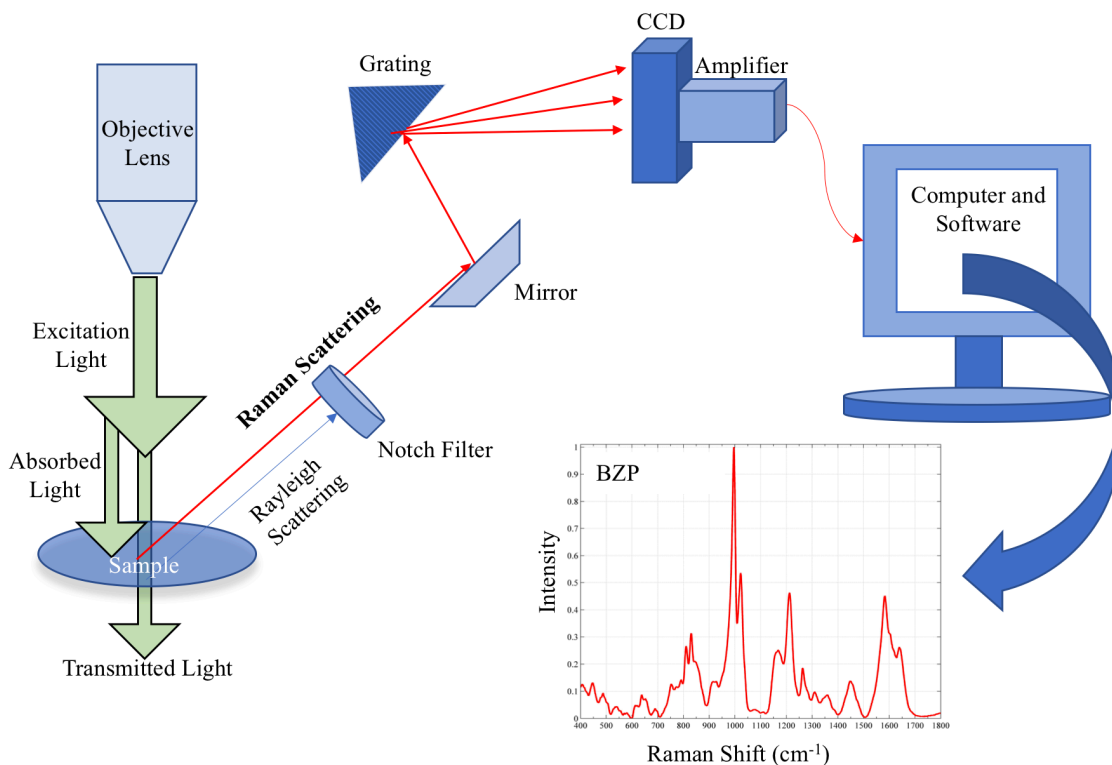


**Figure 4. The path of light in SERS.**

### *1.2.3 Current Uses of Raman Spectroscopy and SERS in Forensic Drug Chemistry*

As Raman spectroscopy is a rapid test with little to no sample prep, it is an attractive method for application in the forensic field, specifically in forensic drug chemistry (18, 22). It has been most utilized for its ability to obtain many spectra in a short amount of time, thus allowing for many samples to be tested. One application of Raman spectroscopy in drug chemistry is called Raman spectral mapping, where Raman spectroscopy is used to test the homogeneity of bulk drug samples. By not only detecting drugs within a sample but also the different adulterants and diluents used, investigators can determine a common origin of bulk powder drug seizures. Different illicit drug

manufacturers will use different combinations and amounts of adulterants and diluents, so comparing these factors can help investigators trace drug distribution networks (18).

Portable Raman spectroscopy can also be used *in situ* to determine drugs in various matrices (22, 23). In one study, researchers were able to determine the presence of the common drug-facilitated sexual assault compound flunitrazepam in both alcoholic and non-alcoholic beverages. Even though bands were always present in the spectra that were caused by the beverage matrix, five characteristic marker bands used to identify flunitrazepam were present in different types of alcoholic beverages with ethanol concentrations up to 40% (23).

More recently, the use of SERS over traditional Raman spectroscopy has been investigated for use in drug chemistry and toxicological studies (13, 24, 25). SERS is sometimes preferred over IR spectroscopy because aqueous solutions can be analyzed; this can be difficult in IR spectroscopy because aqueous solutions have strong water absorption bands in the spectrum. SERS is often preferred over Raman spectroscopy because of its increased sensitivity and the lack of interference from fluorescence, a problem that often presents with normal Raman spectroscopy (13, 24, 25).

As is helpful for many types of chemical instrumentation including GC-MS and IR spectroscopy, there is a push in the field of drug chemistry to build a SERS spectral library (13). As each molecule possesses a unique SERS spectrum, drugs could potentially be identified by matching an unknown spectrum with a known drug spectrum from a library. In 2011, Farquharson and colleagues built a SERS spectral library of over 152 different prescription, over the counter, and illicit drugs, as well as drug metabolites.

Among these 152 drugs, the SERS spectrum of BZP was recorded. No other synthetic piperazine has been analyzed using SERS. These spectra were obtained using SERS-active capillaries, which consist of gold colloids immobilized within a sol-gel matrix and are contained in glass capillary tubes. After a SERS library was built, the researchers spiked drugs in saliva samples and attempted to identify the drugs using a portable SERS instrument. This involved a solid-phase extraction (SPE) step prior to analysis (13).

While SERS has advanced into the field of drug chemistry, most methods involve sol-gel capillaries, which are not as portable or user-friendly as would be desired for field application. This would also be more difficult for instruments used by non-scientists. It was the desire of researchers that future work would develop a simple “lab-on-a-chip” SERS method capable of use by scientists, medical personnel, and law enforcement officials alike (13).

### **1.3 Density Functional Theory**

Although Raman spectroscopy, and thus, SERS, are extremely useful tools in the determining information about the structure of a molecule, assignment of the vibrational modes that produce Raman bands can be complicated (21). Theoretical calculations can help determine which vibrational modes will give rise to certain bands within a Raman or SERS spectrum. One such theoretical approach is the density functional theory (DFT) method. DFT is a computational chemistry method that utilizes quantum mechanical modeling to investigate the electronic structure of a system. The electronic structure of a system in DFT refers to both the location of electrons within a molecule, as well as

correlation of those electrons (26). In the field of forensic drug chemistry, the system in question would be a drug molecule (21).

DFT calculations are carried out using the assumption that the energy of a molecule is a function of its electron density (25, 26). As electron density is also a function, the energy is known as a functional, which is a function of a function. Electron density is a function of three variables: the x-coordinate, y-coordinate, and z-coordinate of the electrons (Equation 3). Therefore, the energy of a molecule would be the function of this function, as displayed in Equation 4 (25, 26).

**Equation 3. Electron density function.**                      ***Electron density =  $f(x, y, z)$***

**Equation 4. Energy functional.**                              ***Energy =  $F[f(x, y, z)]$***

As the mathematical functions used in DFT calculations are complex and involve a large number of variables, they are done using a computer with software designed for DFT calculations. In the first calculation, known as an optimization calculation, a molecular geometry is determined by minimizing the energy in respect to the electron density (Figure 5) (25).

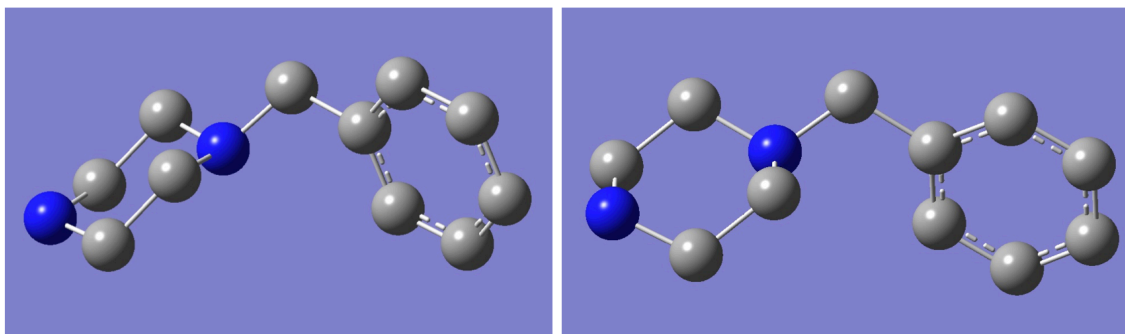


**Figure 5. Results from an optimization calculation of BZP. Image produced in Gaussian 09**

Next, in a vibrational frequency calculation, this molecular geometry is used to obtain the IR and Raman frequencies. These frequencies can be plotted as a theoretical or calculated spectrum, and in the software output, the vibration modes that correspond to each vibrational frequency can be pictured (Figure 6) (25).

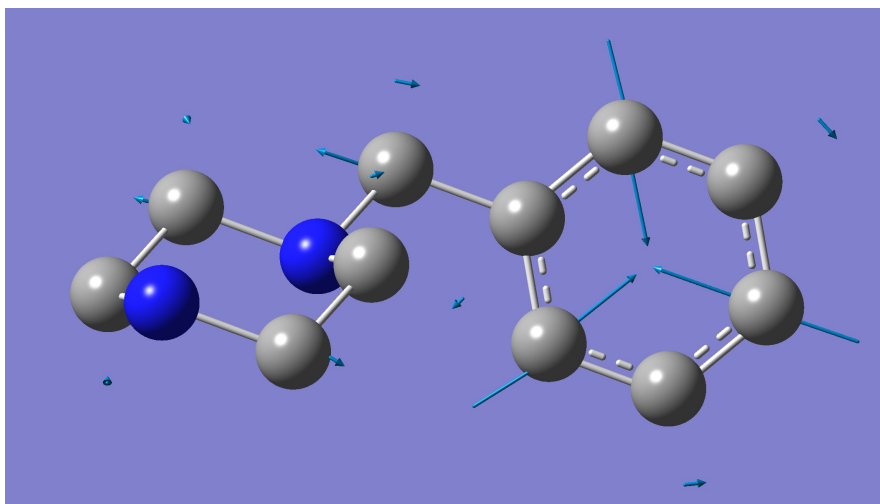


**Figure 6. Result from the frequency calculation of BZP.**

DFT calculations, although not commonly used in forensic science, have been used to analyze experimental data and for spectroscopic study of the interactions between illicit drugs (25). DFT is a powerful tool when used in conjunction with experimental SERS data because it aids the scientists in obtaining a more fundamental understanding of why a spectrum contains particular bands. Being able to recognize these bands, especially when the chemical structure is of a drug molecule is unknown, can help categorize or preliminarily identify the unknown drug.

#### **1.4 Partial Least Squares- Discriminant Analysis with Barcode**

Chemometrics is a field of chemistry that studies the application of statistical analysis to chemical data (27). One common method used in chemometrics is partial least squares-discriminant analysis (PLS-DA). PLS-DA is a linear classification method that combines partial least squares regression with the discriminating power of a classification technique. It determines a mathematical model that is able to classify a sample to its appropriate category or class based on a set of measurements. In its application to spectroscopy, it can be further described as a qualitative method that defines a mathematical relationship between a spectrum (the independent variable) and a class (the dependent variable). Here, each class would represent one drug. A spectrum determined to be in that class would mean the spectrum was identified as that drug (27).

In SERS, the application of PLS-DA allows known drug spectra to be inputs for the PLS-DA software to build a model that would identify a class for each drug represented in the spectral dataset. Then, the model could be used to classify an unknown spectrum and thus determine which drug the spectra is most likely from.

One important step during the construction of a PLS-DA model is cross-validation. (28). Cross-validation involves a series of experiments, also called sub-validation experiments. Each sub-validation experiment involves the removal of a subset of data from the total data set, construction of a PLS-DA model without the removed subset of data, and then the application of this model to the subset of data, testing that data as “unknowns.” This way, the model is built without the data that it then tests. The software takes the unknowns and determines if the PLS-DA model built during the sub-

validation experiment can correctly classify the data. There are multiple types of cross-validation methods; each has a different way of determining how the subset of data is selected. One type of cross-validation is the venetian blinds method. This method will have a number of data splits,  $s$ , that is input by the user. Each subset of data is determined by selecting every  $s^{\text{th}}$  object, therefore, a venetian blind cross-validation will have an  $s$  number of sub-validation experiments (28). Cross-validation serves two functions (27). First, it enables an assessment of the optimal complexity of a model, and second, it allows an estimation of the performance of a model when it is applied to unknown data. A model is considered “invalid” unless it is cross-validated (27).

“Barcode” is a spectral preprocessing, in-house written method coded in MATLAB (MathWorks, Natick, MA) that allows multivariate data analysis techniques, such as PLS-DA, to provide enhanced spectral classification (29). The barcode is based on the sign, positive or negative, of the second derivative of the SERS spectra as a function of Raman frequency. The spectrum is Fourier-filtered prior to this barcoding procedure in order to remove high frequency noise components. An upward curvature in the spectrum (positive second derivative) is assigned as a “+1” and a downward curvature (negative second derivative) is a “0” via this barcoding methodology. The result is that each spectrum is represented as a frequency-dependent binary “fingerprint.” Once processed, the spectra look like barcodes (Figure 7). Without preprocessing using the barcode method, the PLS-DA model may misclassify spectra due to small variations in relative intensities or broad baseline differences. The use of barcoding SERS spectra

before use in a PLS-DA model has been demonstrated to increase specificity and reproducibility using this classification technique (29).

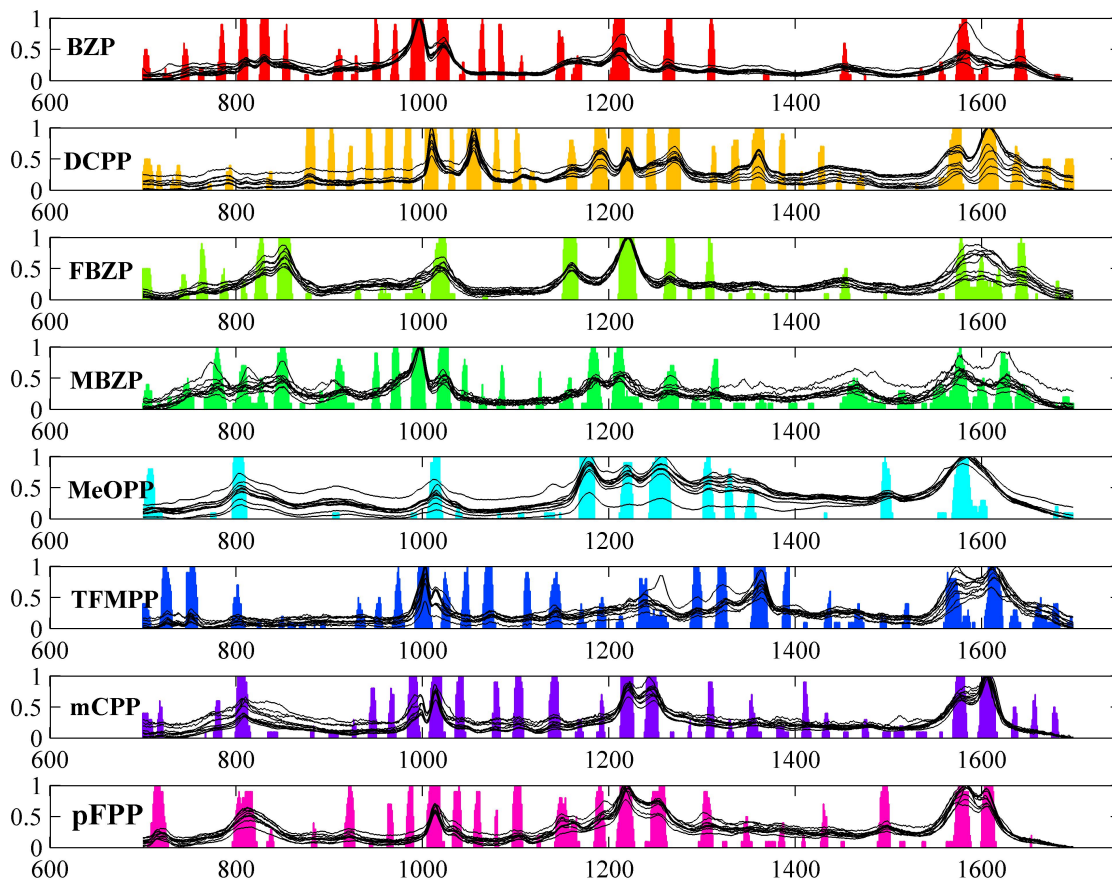


**Figure 7. Visual representative of the Barcode used in PLS-DA with the synthetic piperazines.**  
The raw spectra are in black; the barcodes are in color.

## 2. MATERIALS AND METHODS

### 2.1 Synthetic Piperazines

All synthetic piperazines were purchased from Cayman Chemical Company (Ann Arbor, Michigan) except for mCPP, which was purchased from Cerilliant Corporation (Round Rock, Texas). Derivatives of BZP used in this research are BZP itself, 1-(4-fluorobenzyl)-piperazine (FBZP) and 4-methyl-1-benzylpiperazine (MBZP). Derivatives of 1-phenylpiperazine used in this research are MeOPP, 1-(*para*-fluorophenyl)-piperazine (pFPP), mCPP, 2,3-dichlorophenylpiperazine (DCPP) and TFMPP.

For Raman spectral acquisition of synthetic piperazines in powder form, the powder was placed directly on a sodium chloride salt plate and placed in the instrument. For Raman spectral acquisition of synthetic piperazines in solution, solutions were prepared by dissolving approximately 4 milligrams (mg) of powder into 100 microliters ( $\mu\text{L}$ ) of deionized water, resulting in approximately 40 mg/mL solutions. Since the synthetic piperazines were all in their HCl salt form, they were dissolved in water rather than methanol in order to achieve the most concentrated solutions possible for normal Raman signal acquisition. The solutions were put into quartz glass tubes and their normal Raman spectra were obtained.

For SERS spectral acquisition of synthetic piperazines, BZP and mCPP were purchased as 1.0 mg/mL solutions in methanol. Solutions of the same concentration were made of the remaining synthetic piperazines. All SERS spectra were collected at this concentration unless otherwise noted.

## 2.2 Spectral Acquisition

### 2.2.1 SERS Spectral Acquisition

SERS analysis of synthetic piperazines was performed using a Renishaw Raman microscope (RM 2000, Gloucestershire, England) with a 785 nm diode laser (HPNIR785, Gloucestershire, England) and a Leica microscope attachment (Wetzlar, Germany). SERS spectra were collected over a spectral range of 300-1800  $\text{cm}^{-1}$  using the 50x (0.75 numerical aperture, NA) objective. The laser illumination spot on all samples, which is the focused area of the excitation laser beam, measured approximately 2.5  $\mu\text{m}$  by 25  $\mu\text{m}$ . SERS spectra were collected using approximately 0.5 mW of laser power with a 10 second scan time. The Raman instrument was frequency calibrated for all spectral acquisitions using a silicon wafer as a positive control. Data was collected using Renishaw Windows Based Raman Environment (WiRE) Version 1.3 software.

The SERS substrates used in the qualitative analysis of synthetic piperazines were silicon dioxide ( $\text{SiO}_2$ ) chips covered in gold nanoparticles (Figure 8). They were produced by an *in-situ* growth procedure previously developed by this laboratory (30). The substrates have a surface that is approximately 3 millimeters (mm) in diameter and are covered in small aggregates of monodispersed gold nanoparticles, each approximately 80 nm in diameter.

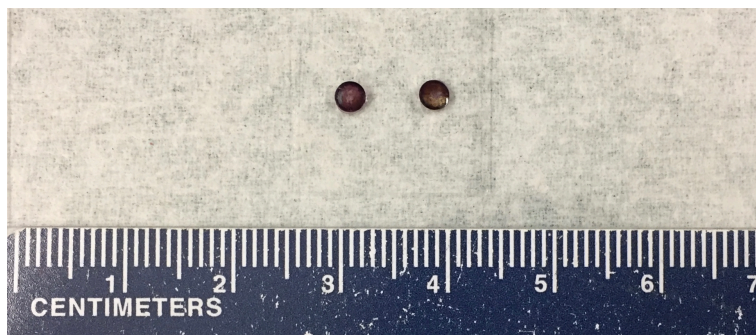


**Figure 8. SERS Substrates.**

One microliter of solution was pipetted on the SERS substrate, left to dry for approximately 5 minutes, and the spectra were then taken. Each SERS spectra reported is an average of 10 spectra, using two separate SERS substrates. Five spectra were taken from each substrate.

Spectral display was conducted using a in-house written code for MATLAB. Pre-processing of the data included a spectral cut ( $400\text{ cm}^{-1}$ - $1800\text{ cm}^{-1}$ ) and normalization of the data, which divides each y-value by the highest y-value for that spectrum. This sets the intensity of the highest band equal to one and the other bands relative to this intensity.

### *2.2.2 Raman Spectral Acquisition*

Raman synthetic piperazine analysis was performed using a Renishaw Raman microscope with a 785 nm diode laser and a Leica microscope attachment. Raman spectra were collected for both synthetic piperazines in powder form and in solution. The normal Raman spectra were taken to compare to SERS spectra as well as to estimate surface enhancement factors (EF). Data for all spectra was collected using Renishaw WiRE software. As the laser power for Raman spectral acquisition was much higher for Raman

than SERS, which can lead to greater background noise and artifacts, a background spectrum was obtained and subtracted from each spectrum.

Raman spectra of synthetic piperazines in powder form were collected by placing approximately 2 mg of the synthetic piperazine powder on a salt plate and placing it under the microscope attachment. The spectra were recorded over a spectral range of 300-3200  $\text{cm}^{-1}$  using the 50x (0.75 NA) objective. The laser spot on the samples measured approximately 2.5  $\mu\text{m}$  by 25  $\mu\text{m}$  and the spectra were collected using approximately 17.5 mW of power with a 10 second scan time.

Raman spectra of synthetic piperazines in solution were collected by placing approximately 100  $\mu\text{L}$  of synthetic piperazines solution into a quartz tube and placing it under the microscope attachment. Spectral data was collected over a spectral range of 300-3200  $\text{cm}^{-1}$  using the 20x (0.40 NA) objective. The laser spot on the samples measured approximately 7  $\mu\text{m}$  by 55  $\mu\text{m}$  and the spectra were collected using approximately 22.5 mW of power with a 180 second scan time.

Due to its Schedule I status, BZP was only available as a 1.0 mg/mL solution and was not purchasable in powder form. This solution was not concentrated enough to produce a Raman signal, so Raman spectra, both in powder and solution, were not obtained for BZP.

As no features of spectral significance were observed below 400  $\text{cm}^{-1}$  or over 1800  $\text{cm}^{-1}$  for SERS spectra, only data from 400-1800  $\text{cm}^{-1}$  is displayed here.

### *2.2.3 DFT Calculations and Theoretical Raman Spectral Acquisition*

DFT calculations were performed using Gaussian 09 (Gaussian, Incorporated, Wallingford, CT). Calculations used a Becke, three-parameter, Yang-Lee-Parr (B3YLP) level of theory with a 6-31G\* basis set. The level of theory and basis set are user-chosen metrics that determine how electron density and correlation is calculated and applied in the software. This combination of level of theory and basis set combination was chosen both because it provides a good balance between accuracy and computational time and because it had been previously published for DFT calculations of controlled substances (25). First, optimization calculations were performed to determine the equilibrium conformation of each synthetic piperazine. This is the physical geometry of the molecule at which it has the lowest energy. Frequency calculations were then performed to determine the theoretical Raman spectrum. The synthetic piperazine's theoretical spectra were calculated for an excitation wavelength of 785 nm, which is the excitation wavelength of the laser used experimentally. The theoretical spectra were exported and processed using MATLAB in the same manner as all other spectra.

To determine band assignments, that is, to determine what molecular vibrations cause which bands within a SERS spectrum, the Gaussian 09 output provides an animation showing molecular vibrational motions corresponding with each band in the theoretical spectrum. The animations were viewed for each band in the DFT spectra, the molecular vibrations were visually determined, and the corresponding bands determined within the SERS, Raman of powder and Raman of solutions spectra for each drug.

## 2.3 Statistical Analysis

### 2.3.1 Enhancement Factors

One common statistic used to estimate the enhancement of SERS signal relative to traditional Raman intensity per molecule is the enhancement factor (EF) (31). The EFs were calculated for each synthetic piperazine by comparing the cross-sections at the most intense band of the SERS spectrum with its corresponding band in the Raman spectrum of that drug in solution. The cross-sections are based on the relative number of molecules within the focus of the laser, the intensities of the bands, the scan times and laser powers. The units for a cross-section is intensity, in counts, per molecule times laser power, in mW, times scan time, in seconds, which is demonstrated in Equation 5 (31).

**Equation 5. Calculation of a cross-section.** 
$$\mathbf{Cross\ section} = \frac{\mathbf{Counts}}{\mathbf{Molecules} \times \mathbf{mW} \times \mathbf{Sec}}$$

To determine the EF of a drug, the SERS cross section of the most intense band was compared with the cross section of the corresponding band in the Raman spectrum (Equation 6).

**Equation 6. Calculation of an enhancement factor.** 
$$\mathbf{EF} = \frac{\mathbf{Cross\ section}_{\mathbf{SERS}}}{\mathbf{Cross\ section}_{\mathbf{Raman}}}$$

For this research, the EF is considered only an estimation because it is difficult to determine the exact number of molecules within the focus of the laser. For the purposes of this estimation, it was assumed that the synthetic piperazine molecules were adsorbed in an even monolayer on the surface of the SERS substrate.

### 2.3.2 PLS-DA Model

Spectral statistical analysis was completed using a PLS-DA toolbox (Eigenvector Research Incorporated; Manson, Washington) for MATLAB after the spectra had been preprocessed using the barcode procedure (29). Ten spectra of each synthetic piperazine were fed into the model as the independent variables and eight classes were made, one for each drug.

The model used a 700-1700  $\text{cm}^{-1}$  spectral range, a Fourier-transforming factor of 60, and 10 latent variables. The model was cross-validated using a venetian blind method with 20 data splits. These parameters were used because they were found to give the best model with the highest sensitivity and specificity of each class, along with the best sensitivity and specificity of the method when unknowns were introduced.

It is important to note that the analytical sensitivity and specificity of a PLS-DA model is separate from the sensitivity and specificity of the SERS method used to build that model.

### 2.3.3 Sensitivity

To determine the sensitivity of this SERS method, that is, how little drug needs to be present to be detected, serial dilutions were performed. Two separate series of dilutions of BZP were made in final concentration of 1000  $\mu\text{g/mL}$ , 500  $\mu\text{g/mL}$ , 100  $\mu\text{g/mL}$ , 50  $\mu\text{g/mL}$ , 10  $\mu\text{g/mL}$ , 5  $\mu\text{g/mL}$  and 1  $\mu\text{g/mL}$ . Five spectra were taken from each concentration in each dilution for a total of 10 spectra per concentration. All spectra were measured using the same SERS method as previously mentioned.

One measure of sensitivity is the limit of detection (LOD). The LOD is the lowest concentration at which spectra can be correctly identified below a specified error rate. To determine the LOD, the 70 spectra (10 from each concentration) were fed into the PLS-DA model as unknowns. The PLS-DA model classified each spectrum into one class to which they most probably belonged. A particular concentration was considered to be correctly identified if it had an error rate of less than or equal to 20%; this would mean that up to two out of the 10 spectra could be misclassified. This error rate was chosen because it is a common acceptable error rate used by the Scientific Working Group for the Analysis of Seized Drugs (SWGDRUG) and the Scientific Working Group for Forensic Toxicology (SWGTOX) when dealing with LOD (32).

#### *2.3.4 Specificity*

To determine the specificity of this SERS method, a blind, “unknown” test was performed. Solutions of each synthetic piperazine were prepared at a concentration of 1.0 mg/mL. A third party randomized the solutions into numbered vials and the identity of each vial was kept unknown to the data collector. Ten spectra of each unknown drug were collected using the same SERS method as above.

To determine the specificity of the method, the unknown spectra were fed into the PLS-DA model to be classified. Each spectrum was classified as one of the eight classes of the PLS-DA model. A drug, as a whole, was considered identifiable with this method if 80% or greater of the spectra were correctly classified. The data were held to a standard

error rate of equal to or less than 20%. This acceptable error rate was chosen because it was the error rate also used for the sensitivity of the method.

### 3. RESULTS AND DISCUSSION

#### 3.1 SERS

##### 3.1.1 SERS Spectra

Eight synthetic piperazines were measured by SERS using SiO<sub>2</sub> chips covered in gold nanoparticles. The interaction with the gold nanoparticles enhanced the Raman scattering for all eight of the synthetic piperazines and SERS spectra were obtained (Figure 9). Ten spectra of each drug were averaged to produce the final spectra, which is a relatively low number of scans to give such a high signal-to-noise ratio. All eight drugs were found to give a robust and repeatable signal using SERS.

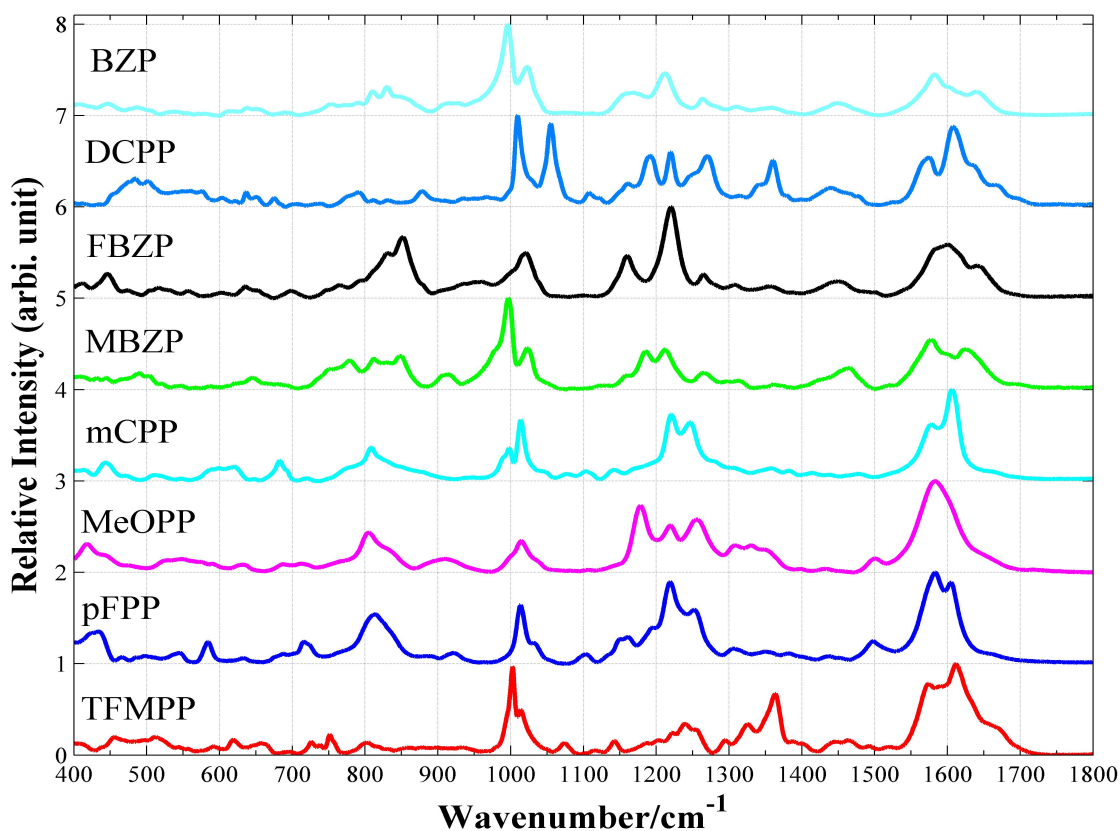
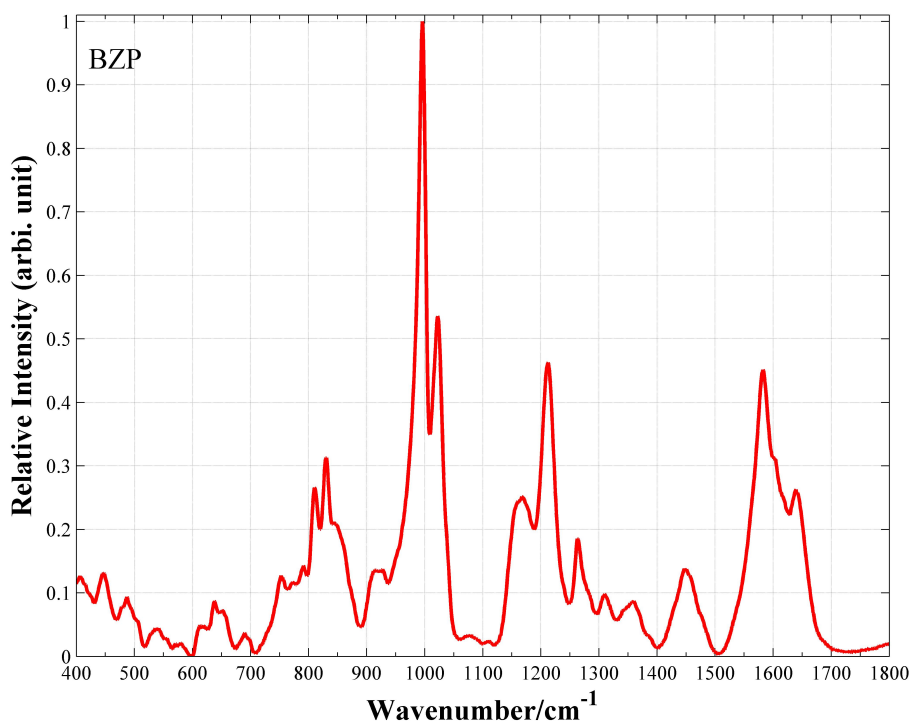


Figure 9. SERS spectra of eight synthetic piperazines

The spectra of the synthetic piperazines are mostly distinguishable by the eye, although they share some common bands due to their similarity in chemical structure. Two common bands present in the eight synthetic piperazines were observed at  $\sim 1000$   $\text{cm}^{-1}$  and  $\sim 1600$   $\text{cm}^{-1}$ ; these are bands commonly found in many illicit drugs that are caused by molecular vibrations in the benzene ring (25). Most of the intense features in all spectra were between 700-1700  $\text{cm}^{-1}$  (Figure 10).



**Figure 10. SERS spectrum of BZP.**

Some distinguishing spectral features between the different synthetic piperazines were noted between 700-900  $\text{cm}^{-1}$  and 1100-1300  $\text{cm}^{-1}$ . These are important to note because they are the bands that could be used to distinguish between the synthetic piperazines. Unsurprisingly, drugs that were more similar in structure than others, such as

BZP and MBZP, which differ by a methyl group, had very similar spectra. By this logic, FBZP would also be expected to have a similar spectrum to BZP and MBZP, but it is actually quite different. This is most likely caused by differences between the electronegativity of the atoms within the molecule. The greater electronegativity, which is essentially how much an atom “pulls” on the electrons shared in the covalent bond of the fluorine atom, would cause a greater change in electron density. DCPD and mCPD differ by only one chlorine atom and have similar equilibrium structures, but their spectra are significantly different from one another, which further supports that the electronegativity of the constituent atoms or functional groups have a great effect on the resulting SERS spectrum.

Overall, the eight synthetic piperazines were successful candidates for use with SERS. While it is known that aromatic compounds are generally more successful when using SERS than aliphatic compounds, the lone pair of electrons on the nitrogen in the piperazine ring is believed to be the key to SERS success in this case (17). As synthetic piperazines and most illicit drugs are aromatic compounds and often contain nitrogen groups with lone pairs of electrons, this suggests that other illicit drugs could be successful when using SERS for analysis due to this characteristic.

### *3.1.2 SERS versus Raman of Synthetic Piperazines in Solution*

To demonstrate the advantage SERS has over traditional Raman spectroscopy, the synthetic piperazines' Raman spectra were also measured. To eliminate as many different

variables as possible, SERS spectra were compared to Raman spectra of synthetic piperazines in solution instead of powder form, as solutions were used in SERS.

While all SERS spectra were measured using drug concentrations of 1 mg/mL, those solutions were not concentrated enough to produce a signal with normal Raman spectroscopy. Solutions of each synthetic piperazine were prepared for Raman spectroscopy at concentrations of approximately 40 mg/mL. Viewing the overlapped SERS and normal Raman spectra, it is evident that SERS produces more intense spectra than normal Raman spectroscopy with more peaks and less noise, all while requiring less of the drug in the sample (Figure 11). Many bands observed in the SERS spectra of these compounds are not present in the corresponding normal Raman spectra, which would lead to lower discriminating power between spectra of different drugs via normal Raman spectroscopy.

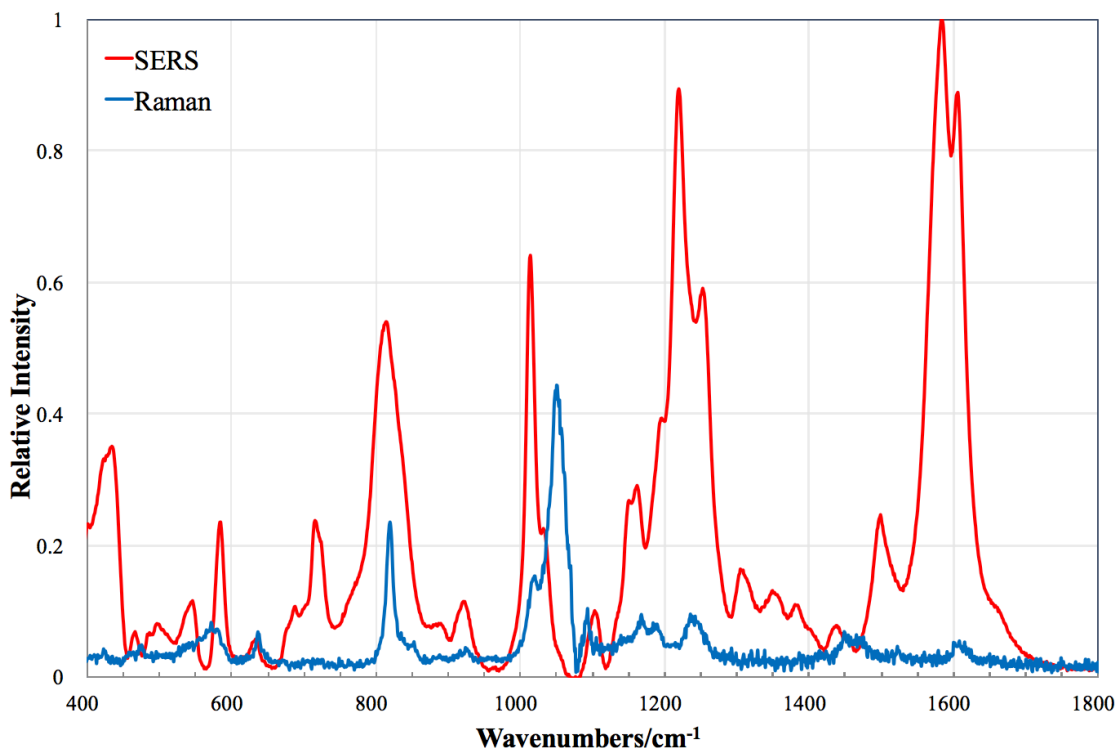


**Figure 11. SERS and Raman spectra of pFPP.**

It is important to note that not only did the concentration of the solution need to be 40 times greater with Raman than SERS, but the method had to be modified as well. To obtain a Raman spectrum with any detail, the laser power and scan time had to be increased (Table 1). A volume of approximately 100  $\mu\text{L}$  was needed for Raman spectroscopy while only 1  $\mu\text{L}$  was needed for SERS. The increase in signal intensity with a decrease in time and required resources demonstrates the clear advantage SERS demonstrates over traditional Raman spectroscopy.

**Table 1. Method differences between SERS and Raman of solutions**

<b>Parameter</b>	<b>SERS</b>	<b>Raman of Solutions</b>
<b>Concentration of Drug</b>	1.0 mg/mL	40 mg/mL
<b>Volume Required</b>	1 $\mu$ L	100 $\mu$ L
<b>Laser Power</b>	0.5 mW	22.5 mW
<b>Scan Time</b>	10 seconds	180 seconds

Although the spectra being compared in Figure 11 are of the same drug, pFPP, the spectra are visibly different in band frequencies and relative intensities. This is expected for many reasons. As the interaction of the incident light with the gold produces a localized plasmon field, the drug molecule's orientation and individual atoms' proximities to the gold nanoparticles will cause shifts in frequency and intensity differences. For example, the largest difference that can be noted in the pFPP spectra is the largest SERS band at approximately  $1600\text{ cm}^{-1}$ . As will be discussed further in the DFT calculation results, this band is common to the synthetic piperazines and is due to molecular in-plane stretching vibrations in the benzene ring. This suggests that the vibrational modes in the benzene ring were either closer to the surface of the SERS substrate or had vibrational modes with polarization components perpendicular to the surface. It is not an issue that the SERS spectra are different from the Raman spectra because an unknown SERS spectrum would only be compared against a SERS library.

### *3.1.3 Raman of Synthetic Piperazines in Power Form*

To determine if SERS would be advantageous over traditional Raman spectroscopy when analyzing a synthetic piperazine in solid dose form, Raman spectra of the synthetic piperazines available in powder (all but BZP) were acquired. In general, having a chemical in solid form would produce a signal strong enough for Raman spectroscopy. For Raman spectroscopy, the powders were placed on reusable salt plates. These salt plates would not be as feasible in field work as SERS substrates because they are costly, fragile and would need to be cleaned in between uses. In contrast, this lab's method of producing SERS substrates costs only cents per substrate and the substrates can be disposed of once a sample has been analyzed. By not having to reuse a drug sample in multiple tests, this would help prevent the contamination of subsequent samples. Raman spectroscopy for the synthetic piperazine powders required more laser power than SERS (17.5 mW compared to 0.5 mW, respectively). In the field, a less powerful laser would be desired because it would require less battery power, meaning the portable instrument could last longer on a single charge. More powder was also required for Raman spectra to be obtained. SERS only required 1  $\mu$ L of a 1.0 mg/mL solution, which is only 0.001 mg of powder; Raman required closer to 2 mg. While using as little drug as possible during analysis will always be advantageous, specific situations which would warrant such rationing for trace and residue analysis include if some of the sample was needed for further analysis, or if enough should be kept for the defense to do independent testing.

### 3.2 DFT Calculations and Band Assignments

DFT calculations were performed for all eight synthetic piperazines to help assign the bands observed within the SERS spectra to particular vibrations within the molecule. Overall, the theoretical spectra generated by the DFT calculations were in close agreement with the experimental SERS spectra, especially for the most intense bands. The DFT theoretical spectra had many more bands than SERS, which is a phenomenon noted by researchers who have compared DFT theoretical spectra to experimental data (25).

For all of the synthetic piperazines, the optimization calculation showed the molecule's lowest energy geometry to be with a planar benzene ring, including any constituents, and the piperazine ring in a chair or boat conformation. For BZP, its lowest energy conformation was with a planar benzene ring and a piperazine ring in a chair conformation (Figure 12). The other synthetic piperazines with planar benzene rings and piperazine rings in chair conformation were MBZP, mCPP, MeOPP, pFPP, and TFMPP. DCPP and FBZP instead showed boat conformations of their piperazine ring portion.

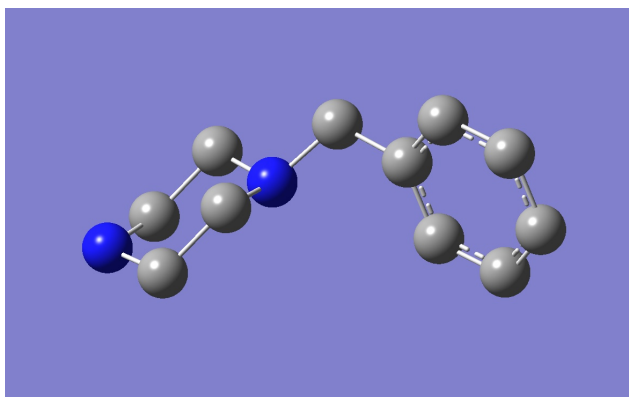


**Figure 12. Lowest energy conformation of BZP.**

In the SERS spectrum of BZP, intense bands were observed at 810, 830, 996, 1023, 1174, 1213, 1264, 1444, and 1581  $\text{cm}^{-1}$ . In the DFT-calculated spectrum, those bands were observed at 785, 798, 1015, 1028, 1163, 1237, 1259, 1463, and 1627  $\text{cm}^{-1}$ , respectively (Figure 13).

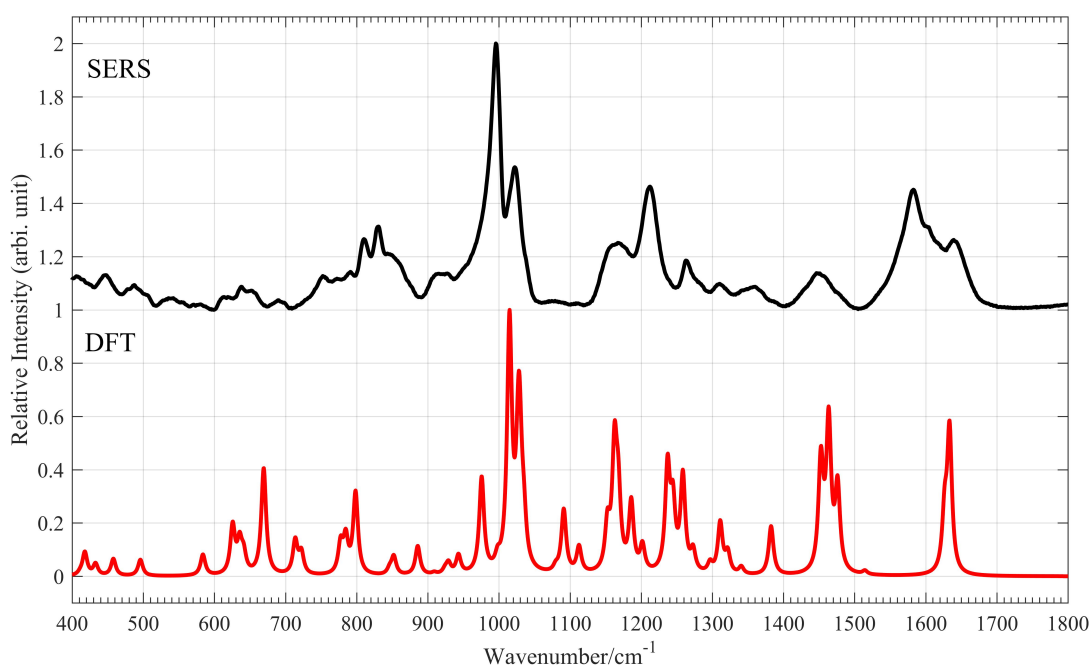


**Figure 13. Comparison of BZP spectra from SERS and DFT calculations**

In BZP, as well as the other synthetic piperazines, as the wavenumbers, and thus energy, increased, so did the difference between the observed and calculated vibrational frequencies. This is likely due to the fact that the DFT calculations are performed using a variational method, and thus calculated energies are expected to be greater than or equal to physical energies (25). Additional differences may arise because the calculations are

performed assuming that the molecule is in the gas phase, where the SERS spectra were recorded from solutions (25). The DFT calculations were also run using the free base form of the molecule where experimentally, the HCl salt forms were used, which could also contribute to the differences between the DFT theoretical and observed normal Raman and SERS spectra. Lastly, the presence of the plasmonic field presents an additional perturbation to the energies and intensities in the SERS spectrum that is not easily accounted for in DFT calculations (25).

Using the Gaussian 09 software, the bands were assigned to the movement of vibrational modes within different parts of the molecule. The three most intense SERS bands of BZP were at 996, 1023 and 1581  $\text{cm}^{-1}$ . It was determined that these bands were mostly due to the bending and stretching of bonds within the benzene portion of the drug, designated in Table 2 as a subscript “C,” (Figure 14).

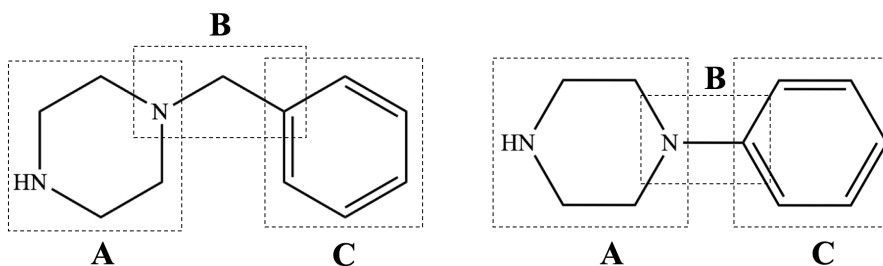


**Figure 14. The letter designations used for the parts of the molecules.** A is the piperazine ring and any of its constituents. B is the group of molecules that connect the piperazine ring to the benzene ring. C is the benzene ring and any of its constituents.

**Table 2. Band assignments for BZP.**

<b>SERS (cm<sup>-1</sup>)</b>	<b>DFT (cm<sup>-1</sup>)</b>	<b>Description<sup>†</sup></b>
810	785	$\gamma(\text{CH})_C$
830	798	$\nu(\text{CC})_B, \delta(\text{C}=\text{C}-\text{C})_C$
996	1015	$\delta(\text{C}=\text{C}-\text{C})_C$
1023	1028	$\nu_a(\text{CNC})_A, \delta_t(\text{CH}_2)_B, \nu_s(\text{C}=\text{C}-\text{C})_C$
1174	1163	$\delta_t(\text{CH}_2)_B, \nu(\text{CC})_A, \delta_t(\text{CH}_2)_A$
1213	1237	$\delta_t(\text{CH}_2)_A, \delta_t(\text{CH}_2)_B, \nu(\text{CN})_B$
1264	1259	$\delta_t(\text{CH}_2)_A, \delta_w(\text{CH}_2)_A, \delta_w(\text{CH}_2)_B$
1444	1463	$\delta_s(\text{CH}_2)_B, \delta_s(\text{CH}_2)_A$
1581	1627	$\nu_a(\text{C}=\text{C}-\text{C})_C, \delta(\text{CH})_C$

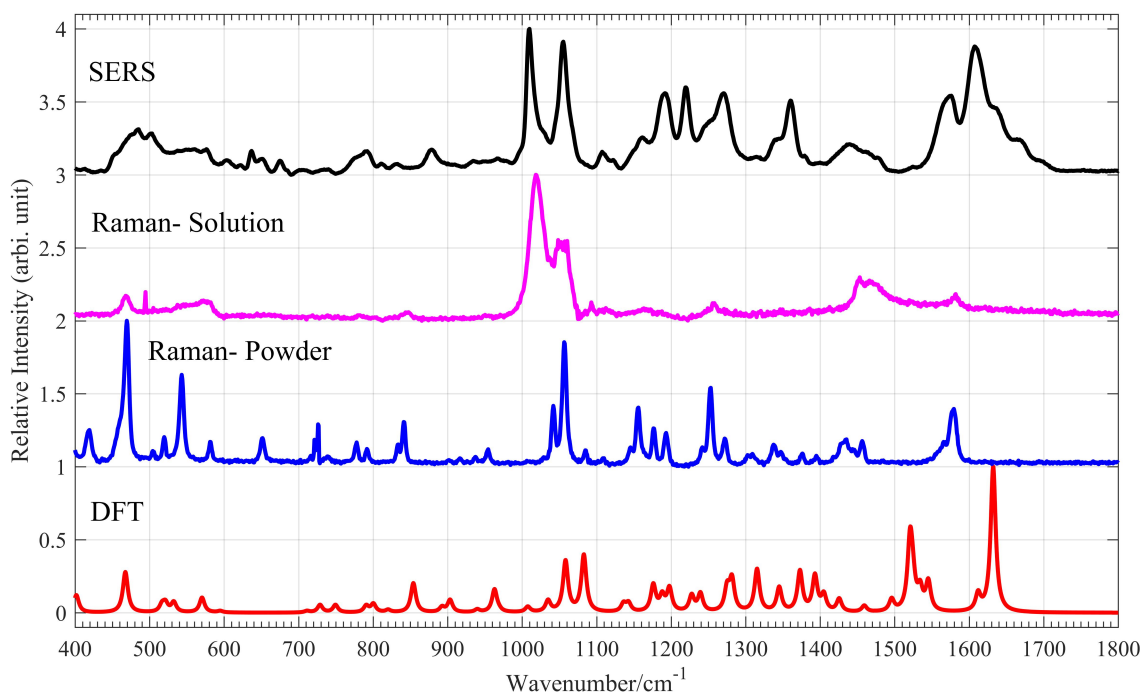
It is well known that benzene and its derivatives show bands around 1000 and 1600 cm<sup>-1</sup>, which was also experimentally observed in all the synthetic piperazines (33). What aids in the differentiation between these molecules are the effects of the atoms and bonds attached to the benzene ring, as these constituents change the electron density and mass distribution within the molecule, which influence the vibrational frequencies and intensities of the SERS spectrum.

These constituents could provide the vibrational modes that give rise to characteristic vibrational marker bands. Characteristic marker bands would be bands observed in a SERS spectrum that would be unique to that molecule when compared to SERS spectra of similar molecules. In the case of the synthetic piperazines, most

---

<sup>†</sup>  $\nu$ , stretching;  $\nu_a$ , asymmetric stretching;  $\nu_s$ , symmetric stretching;  $\nu_b$ , ring breathing;  $\delta$ , bending;  $\gamma$ , out-of-plane bending;  $\delta_s$ , scissoring;  $\delta_w$ , wagging;  $\delta_t$ , twisting;  $\delta_r$ , rocking; A, piperazine ring; B, between rings; C, benzene ring. These notations will be used for all band assignment tables.

displayed a doublet band around  $1000\text{ cm}^{-1}$  where the band at a higher wavenumber was significantly less intense than the band at the lower wavenumber. In the DFT and SERS spectra of DCPD, however, the two bands were slightly farther from each other and much closer in intensity (Figure 15). For this reason, it could be proposed that the band observed at  $1055\text{ cm}^{-1}$  in the SERS spectrum of DCPD and the corresponding band at  $1083\text{ cm}^{-1}$  in the DFT spectrum could be a characteristic vibrational marker band for DCPD (Table 3).

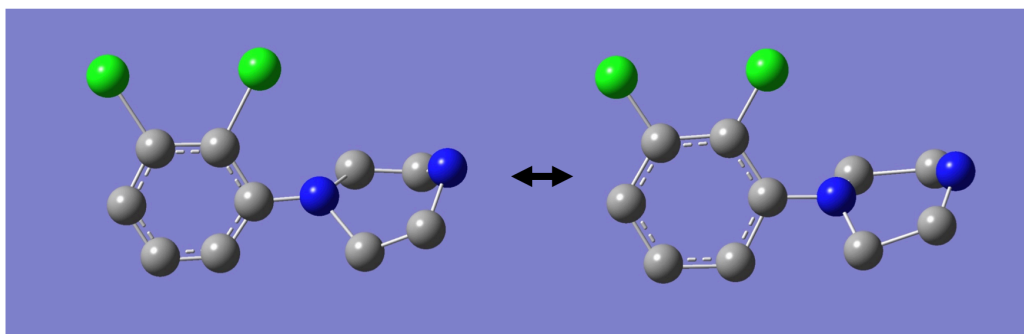


**Figure 15. All DCPD spectra.**

**Table 3. Band assignments for DCP<sup>‡</sup>**

SERS (cm <sup>-1</sup> )	Raman-Solution (cm <sup>-1</sup> )	Raman-Powder (cm <sup>-1</sup> )	DFT (cm <sup>-1</sup> )	Description
475	468	469	467	$\delta(\text{CCl})_C$ , $\nu(\text{CCl})_C$ $\delta(\text{CNC})_A$
503		504	517	$\gamma(\text{C=C-C})_C$ , $\delta(\text{CCl})_C$
1010	1019	1042	1058	$\delta(\text{C=C-C})_C$ , $\nu(\text{CCl})_C$
1055	1061	1057	1083	$\nu_b(\text{C=C-C})_C$ , $\nu(\text{CCl})_C$ , $\delta_r(\text{CH}_2)_A$
1191		1155	1198	$\delta(\text{CH})_C$ , $\nu_a(\text{CNC})_A$ , $\delta_r(\text{CH}_2)_A$
1220		1193	1281	$\delta_t(\text{CH}_2)_A$
1272	1256	1253	1315	$\nu_a(\text{C=C-C})_C$ , $\delta(\text{CN})_B$ , $\delta(\text{CH})_C$ , $\delta(\text{CCl})_C$
1361			1373	$\nu(\text{CN})_B$ , $\delta_w(\text{CH}_2)_A$ , $\delta(\text{CH})_C$ , $\delta_t(\text{CH}_2)_A$
1572			1612	$\nu_a(\text{C=C-C})_C$ , $\delta(\text{CH})_C$ , $\delta(\text{CN})_B$ , $\delta(\text{CCl})_C$
1608	1582	1578	1632	$\nu_a(\text{C=C-C})_C$ , $\delta(\text{CH})_C$ , $\delta(\text{CCl})_C$

By analyzing the frequency calculation, it was determined that the dominant vibrations associated with the 1055 cm<sup>-1</sup> SERS peak were the breathing of the benzene ring and stretching between the benzene ring and chlorine atoms (Figure 16).

**Figure 16. The DCP<sup>‡</sup> vibrational mode at 1083 cm<sup>-1</sup>.**

<sup>‡</sup> Not all corresponding bands from the SERS spectrum were present in the traditional Raman spectra. For this reason, there are some band locations that are purposefully left blank in the table because these bands did not exist in that spectrum.

### 3.3 Statistical Analysis

#### 3.3.1 Enhancement Factors

Using the cross sections from the largest band in the SERS spectrum and its corresponding band in the Raman spectrum of each synthetic piperazine, an EF was calculated for each drug (Table 4).

DCPP had the lowest EF at  $10^6$  and mCPP, MeOPP, and TFMPP had the highest, which each demonstrated an EF of  $10^8$ . The Raman scattering from these three drugs, enhanced by the gold nanoparticle SERS substrates, was as great as eight orders of magnitude larger than the signal from Raman scattering without surface enhancement, taking into account all the parameters of the method. The range in EFs could be caused by the differences in molecular geometry between the synthetic piperazines, as it is known Raman scattering is more strongly enhanced for vibrational modes that have polarization components perpendicular to the surface (17, 21). In fact, the two drugs with their piperazine rings in a boat conformation, DCPP and FBZP, demonstrated lower EFs.

**Table 4. Enhancement factors of synthetic piperazines.**

<b>Drug</b>	<b>EF</b>
DCPP	$10^6$
FBZP	$10^7$
MBZP	$10^7$
mCPP	$10^8$
MeOPP	$10^8$
pFPP	$10^7$
TFMPP	$10^8$

### 3.3.2 PLS-DA Model

Using ten spectra from each synthetic piperazine at a concentration of 1.0 mg/mL, a PLS-DA model was created (Figure 17). The model had eight classes, one for each synthetic piperazine. The model was cross-validated using the venetian blinds method, which allowed for an estimation of the performance of the model when it was applied to unknown data.

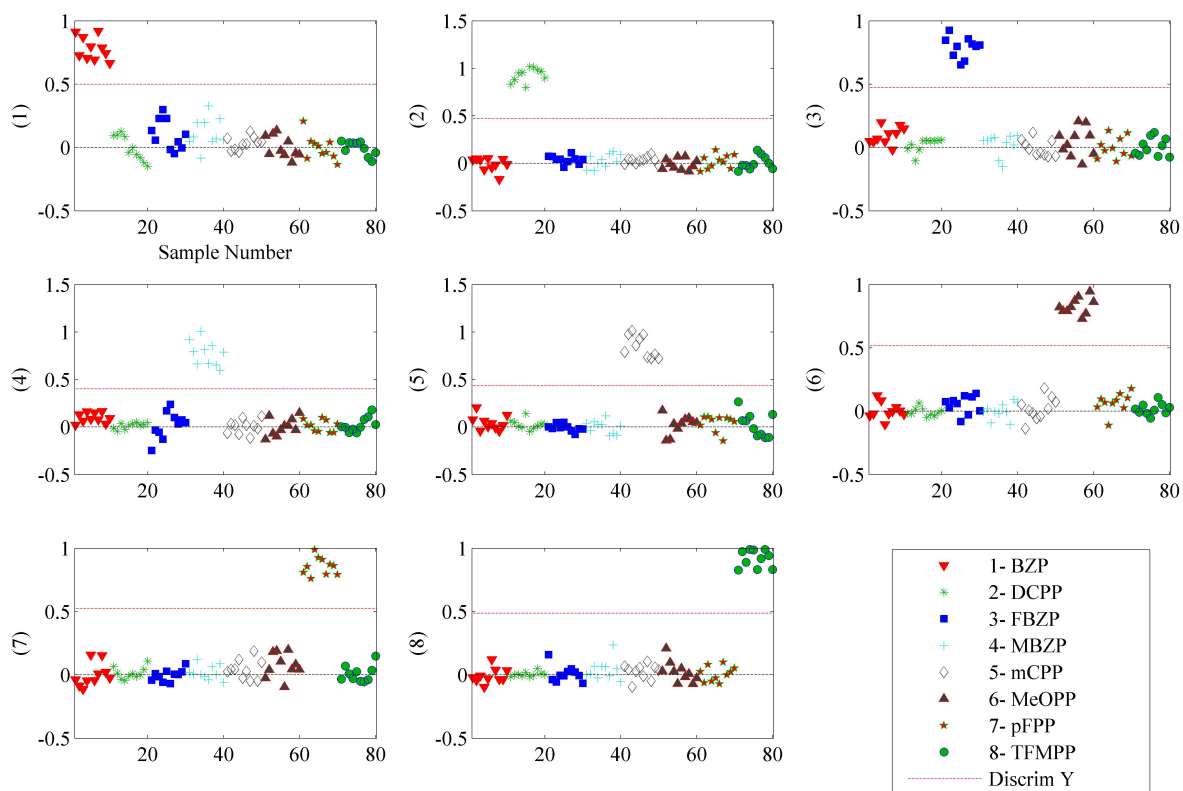


Figure 17. PLS-DA prediction value plots.<sup>§</sup>

<sup>§</sup> The 80 spectra were represented on the x-axis as sample value. For a sample to be predicted as belonging to a particular class (y-axis), it must be over the discriminating red line. For example, in the top left plot, Samples 1-10 are predicted to belong to Class 1, or BZP.

Two measures of strength of a PLS-DA model are sensitivity and specificity. Statistically speaking, sensitivity is defined as the true positive fraction (34). During cross-validation, the software randomly takes spectra, creates a model without these spectra, builds a model, then feeds them into the model as “unknowns.” A high sensitivity would mean that the unknowns were predicted to belong to a class and truly belonged to that class, thus being true positives. For example, if all ten spectra of BZP were chosen during cross-validation and tested as “unknowns,” a sensitivity of 100% would mean that all ten spectra were correctly classified as BZP. Specificity is statistically defined as the true negative fraction (34). During cross-validation, a high specificity would mean that if spectra were chosen and were determined not to belong to a particular class, that they truly did not belong in that class. For example, for the BZP class to have a high specificity, any spectra that were not BZP during cross-validation would have to not be classified incorrectly as BZP. In this model, all eight classes were determined to have 100% specificity and 100% sensitivity, meaning that all spectra were correctly classified during cross-validation. It is important to note that the analytical sensitivity and specificity of the PLS-DA model are different from the sensitivity and specificity of the SERS method, as discussed below.

### *3.2.3 Sensitivity*

The PLS-DA model was used to determine the sensitivity of the SERS method by determining the LOD. To determine the LOD, two serial dilutions of BZP were performed and five spectra from each concentration in each dilution were fed into the

PLS-DA model as unknowns. Although this method of determining the sensitivity is strict and could produce a higher limit of detection than other methods, the PLS-DA model was used because PLS-DA has the potential to be an algorithm used in a portable SERS instrument to rapidly identify novel psychoactive substances and other drugs.

Visually, it appears that the SERS spectra of BZP maintain most of the characteristic bands throughout the dilution, although the signal-to-noise ratio decreases, which is expected (Figure 18). Around 10  $\mu\text{g/mL}$ , certain spectral features change, including the bands observed between 800 and 900  $\text{cm}^{-1}$  and a shift in the bands observed between approximately 1150 and 1250  $\text{cm}^{-1}$ .

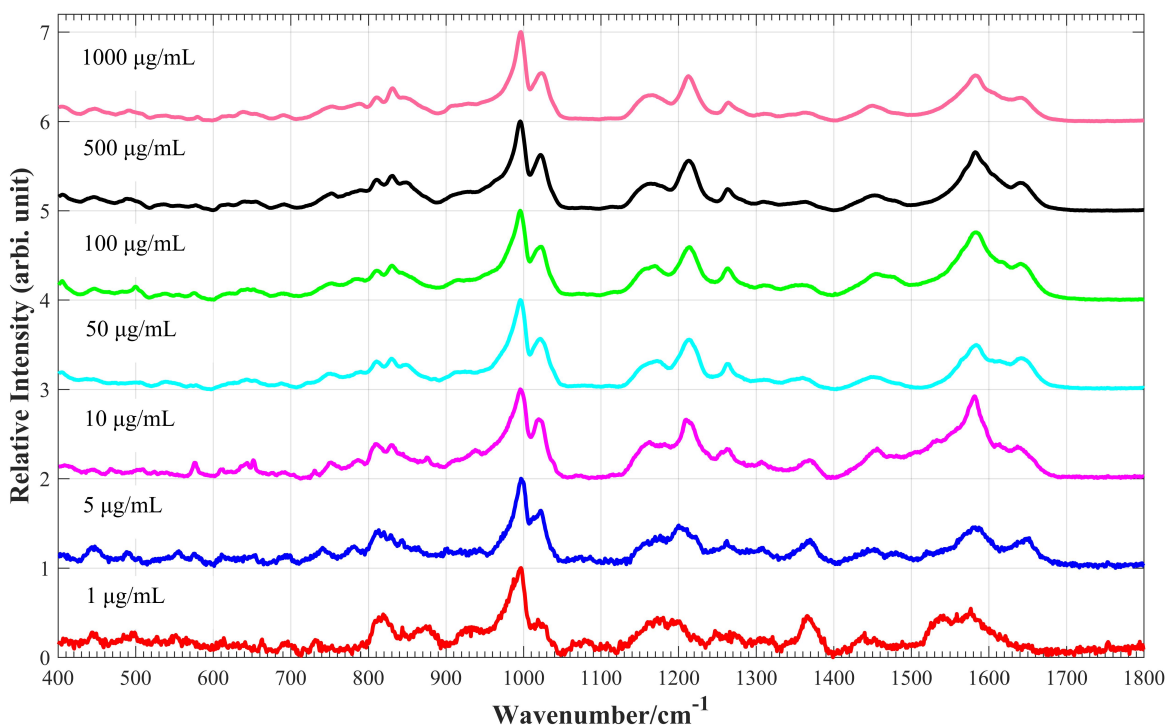


Figure 18. SERS spectra from BZP dilutions

The LOD for BZP was determined to be 10 µg/mL. At this concentration, the error rate was 10%, which was considered acceptable. Below this concentration at 5 µg/mL and 1 µg/mL, the error rate rose to 60% and 80%, respectively (Table 5).

**Table 5. Error rates from BZP dilutions.**

<b>Concentration</b>	<b>Error Rate</b>
<b>1000 µg/mL</b>	0%
<b>500 µg/mL</b>	0%
<b>100 µg/mL</b>	10%
<b>50 µg/mL</b>	0%
<b>10 µg/mL</b>	10%
<b>5 µg/mL</b>	60%
<b>1 µg/mL</b>	80%

Although a lower LOD is always desirable to demonstrate higher sensitivity, this is an adequate starting location. In a drug seizure, the analyst can control the amount of drug used during testing, so a lower LOD is not necessarily required. The LOD would be more of a concern if this method was used for toxicological testing, as different drugs in biological fluids are often found in concentrations in the ng/mL range and even lower.

#### 3.2.4 Specificity

In a blind test of all eight synthetic piperazines, ten spectra were taken of each drug and fed into the PLS-DA model to be classified. Of the eight synthetic piperazines tested, all were classified with an error rate below 20% (Table 6). Six of those eight drugs had an error rate of 0%. Overall, 78 of 80 spectra were correctly classified, which is a total error rate of 2.5%.

**Table 6. Error rates from the blind test.**

<b>Drug</b>	<b>% Error</b>
<b>BZP</b>	0
<b>DCPP</b>	10
<b>FBZP</b>	0
<b>MBZP</b>	0
<b>mCPP</b>	0
<b>MeOPP</b>	0
<b>pFPP</b>	0
<b>TFMPP</b>	10

This high specificity demonstrates that while the spectra of each synthetic piperazine share common spectral features due to their similarities in chemical structure, they are easily distinguishable from one another using this PLS-DA statistical model.

## **4. CONCLUSIONS**

### **4.1 Future Direction**

This research is only the beginning for the detection of synthetic piperazines using SERS and there are many different directions in which the research could go.

First, the synthetic piperazines were only measured using non-portable instrumentation. These drugs should be tested using the same substrates and method parameters, but on a portable instrument. It would be important to note if synthetic piperazines are as successful on a portable instrument and if any parameters would need to be adjusted.

The issue of sensitivity should be addressed for synthetic piperazines. Although, as mentioned, the LOD is not as crucial in drug chemistry as it is toxicology, SERS could have many applications in the toxicology field and increasing the sensitivity of SERS with the use of synthetic piperazines would be beneficial. Increasing the sensitivity could be evaluated in different ways, such as adjusting the chemometrics applied to the data.

Although this SERS method had high specificity using PLS-DA, these drugs were only researched in their pure form. As many novel psychoactive substances, including synthetic piperazines, are sold as mixtures, and it should be evaluated if individual synthetic piperazines can be identified when they are mixed with other synthetic piperazines, adulterants, diluents, or other drugs.

Ultimately, this SERS method should be evaluated further for its application in the field of forensic toxicology. Driving under the influence of drugs is a major issue facing society and SERS has the potential to be as valuable as an alcohol breath analyzer

in determining if a driver is under the influence. To use SERS for this purpose, oral fluid would first have to be analyzed by itself to determine what bands would be present from the matrix. Then, synthetic piperazines should be spiked into the oral fluid to determine if synthetic piperazines could be identified in oral fluid at various concentrations.

#### 4.2 Evaluation of the Method

Within this research, SERS consistently showed advantages over traditional Raman spectroscopy of synthetic piperazines in powder form or in solution. When visually comparing the spectra, Raman spectra showed lower signal-to-noise ratios, decreased band intensity and a loss of many spectral features (Figure 19).

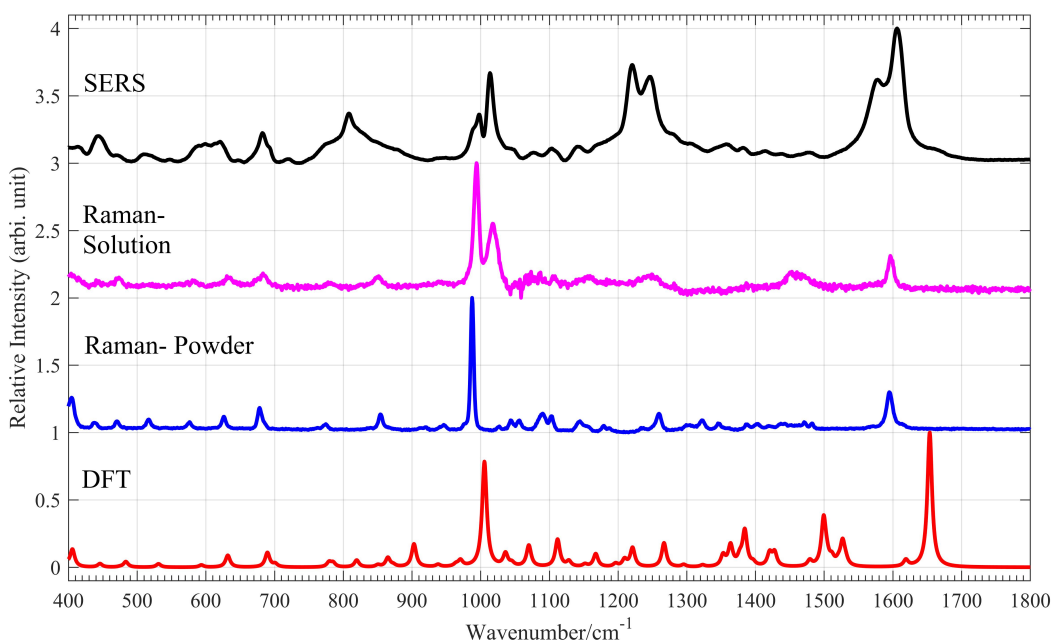


Figure 19. All mCPP spectra.

In comparison to other research using SERS to analyze drugs, this method demonstrated increased sensitivity, as this method required less drug, less laser power, and shorter scan times than many of the research published (13, 24, 25). This method also provided the “lab-on-a-chip” concept other researchers have discussed as part of their future work.

One difficulty that arose during this research was the production of SERS substrate chips. Although overall these chips showed good gold nanoparticle coating, sometimes a batch of chips would be made that were either over-coated or undercoated. This increased the time required for analysis because it took longer to locate the areas with the best coating under the microscope. The difference in coating between chip batches also led to ranging intensities for drug solutions of the same concentration. While this wasn't a large concern for qualitative analysis, obtaining consistent intensities for the same concentration would be vital in quantitative analysis. Data was still collected that demonstrated EFs as high as  $10^8$ , which shows that these SERS substrates are more sensitive than many others being used when factoring in other method parameters (13).

Through the application of PLS-DA to the SERS spectra of synthetic piperazines, it was demonstrated that these drugs could be rapidly identified by a computer system, instead of needing to be identified visually by picking characteristic marker bands for each drug. This ease in identification would be important for the application of portable SERS or in the case where a non-scientist was performing the analysis.

Through this research, it has been demonstrated that SERS can be applied efficiently as a qualitative technique for the analysis of synthetic piperazines. Its

efficiency comes from the requirement of minimal to no sample preparation, the small amounts of drug required to produce a spectrum, the low number of scans required to produce a high signal-to-noise ratio, and the low laser power needed.

## APPENDIX A:

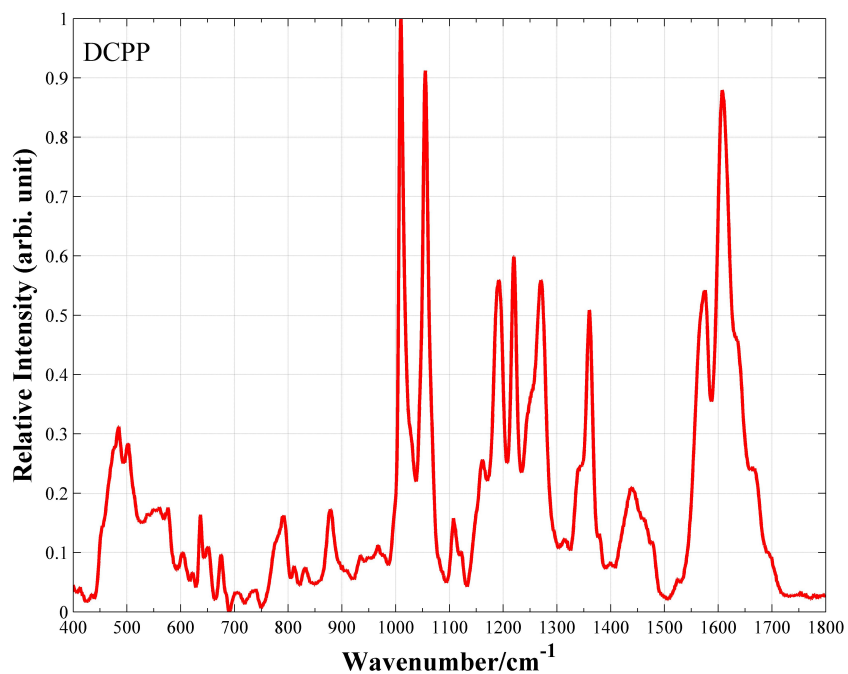


Figure 20. SERS Spectrum of DCPD

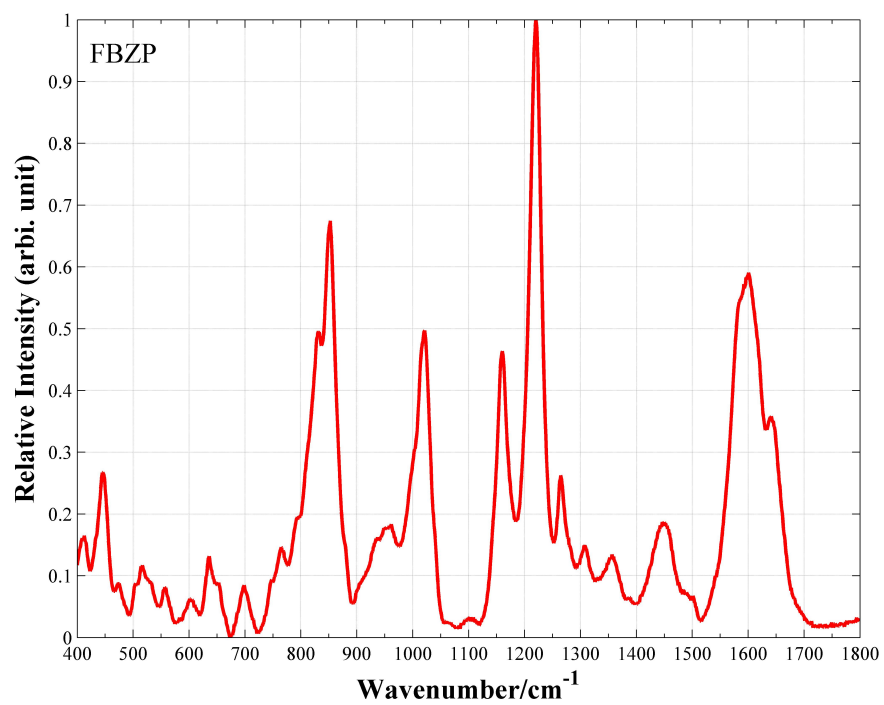


Figure 21. SERS Spectrum of FBZP

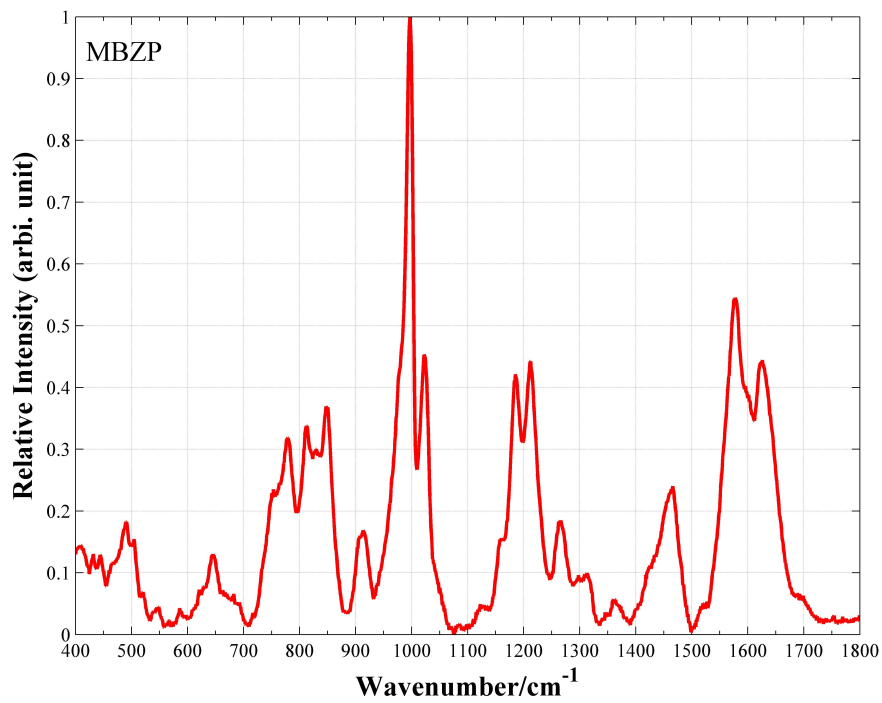


Figure 22. SERS Spectrum of MBZP

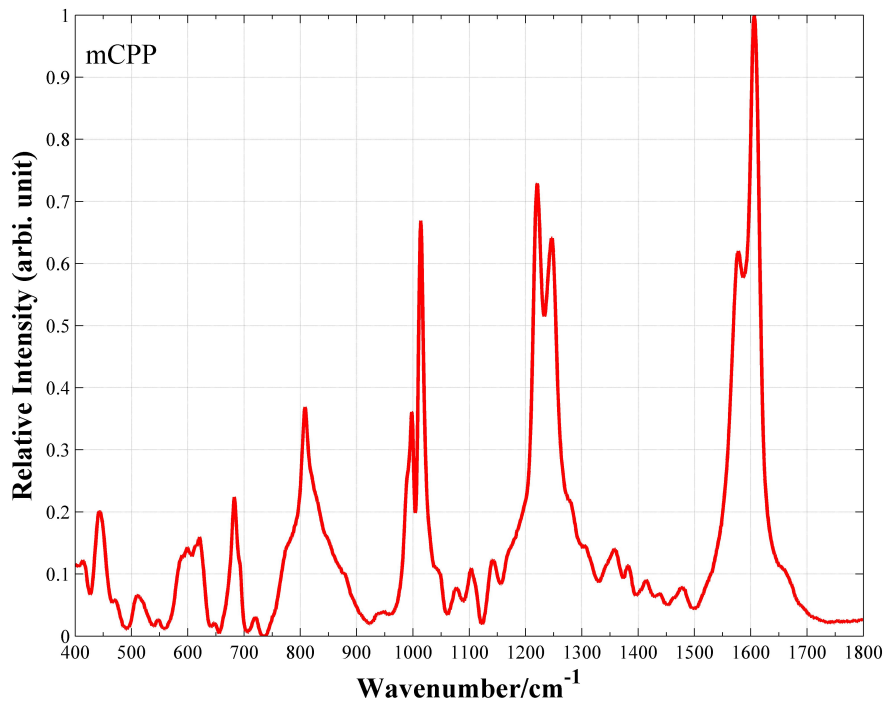


Figure 23. SERS Spectrum of mCPP

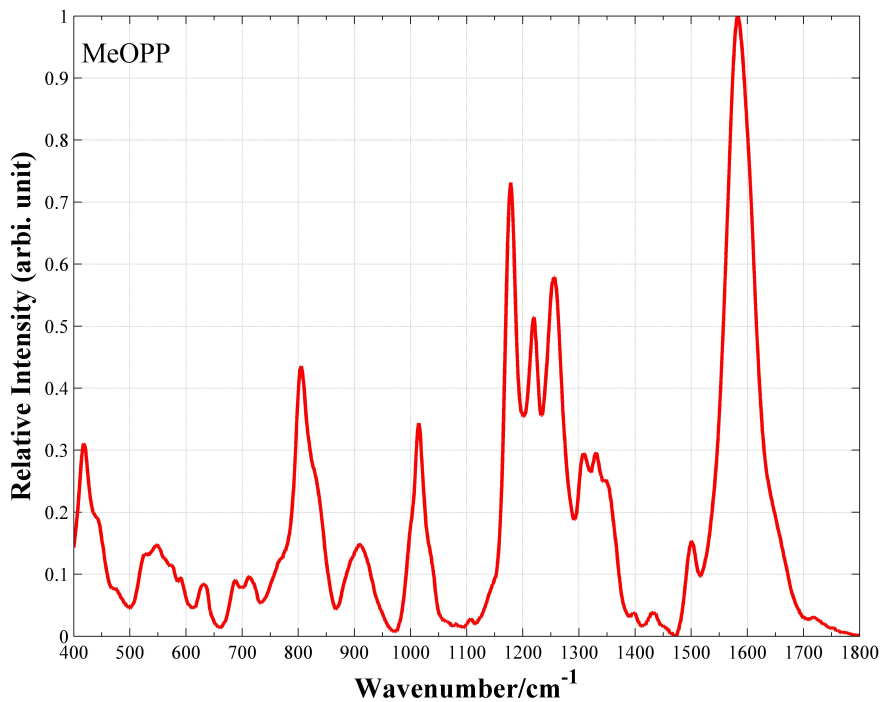


Figure 24. SERS Spectrum of MeOPP

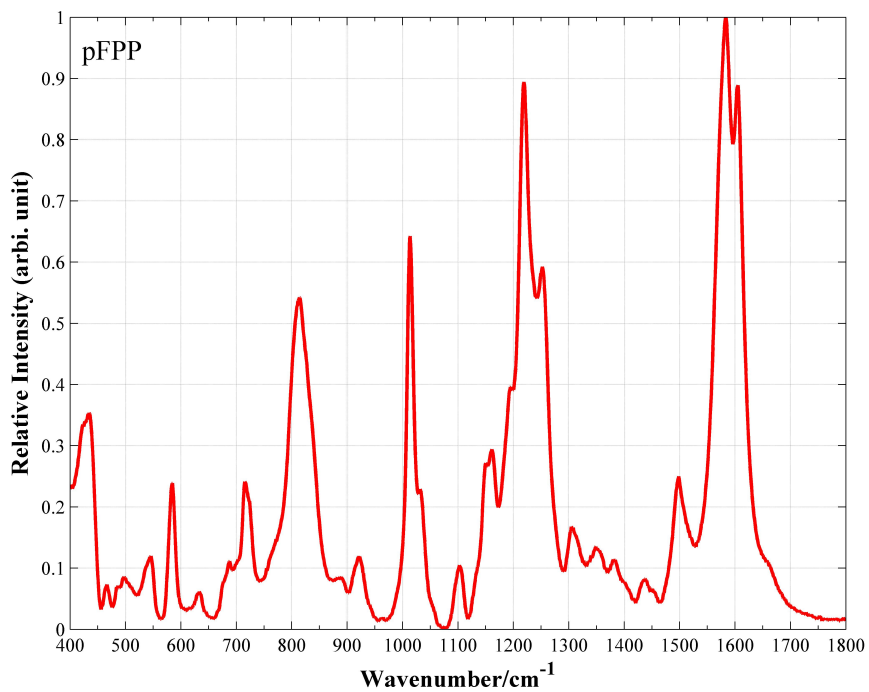


Figure 25. SERS Spectrum of pFPP

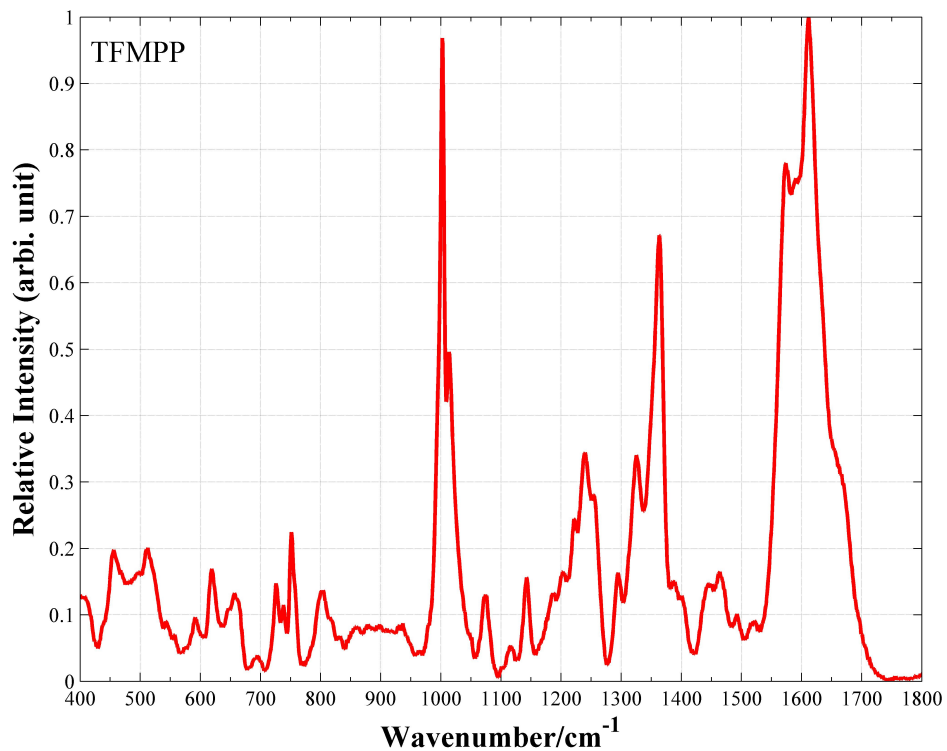


Figure 26. SERS Spectrum of TFMPP

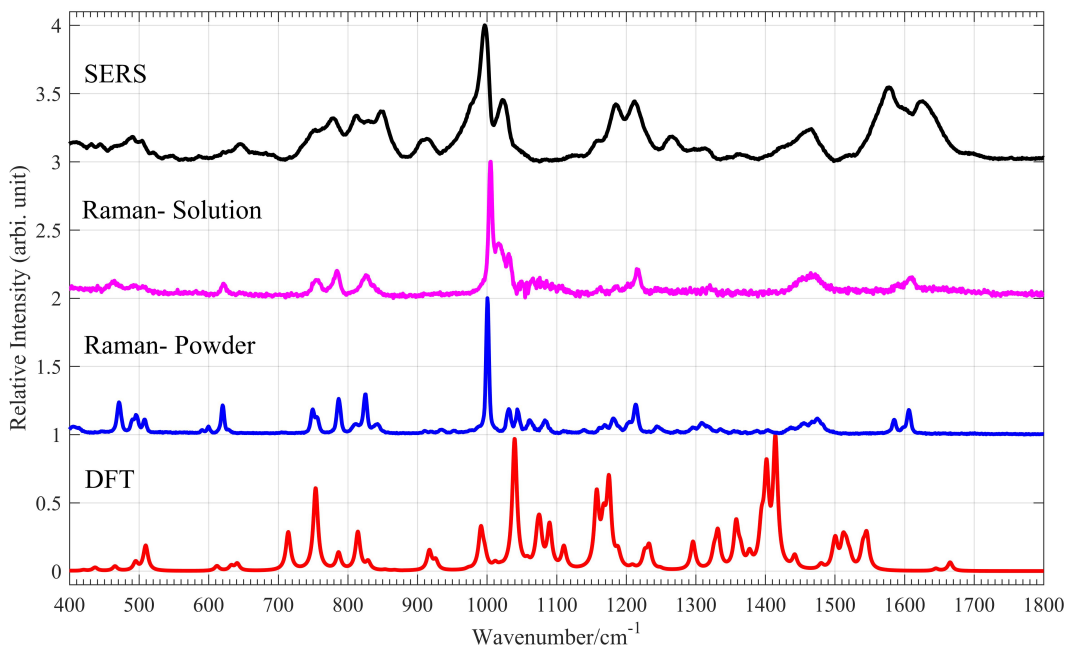
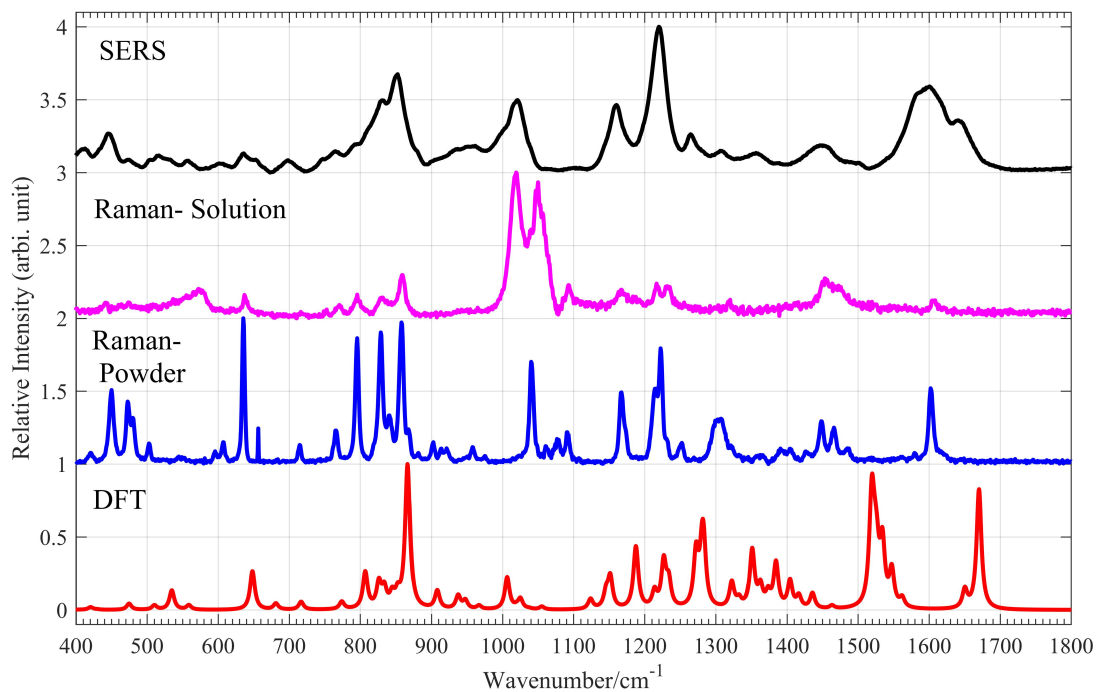
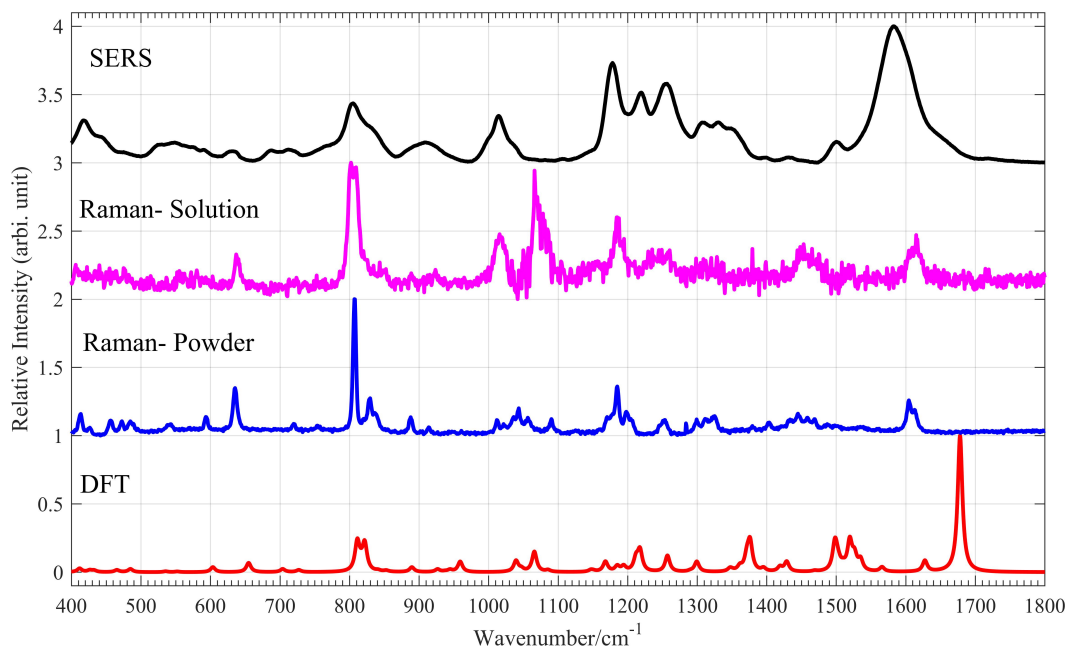


Figure 27. All MBZP spectra



**Figure 28. All FBZP spectra**



**Figure 29. All MeOPP spectra**

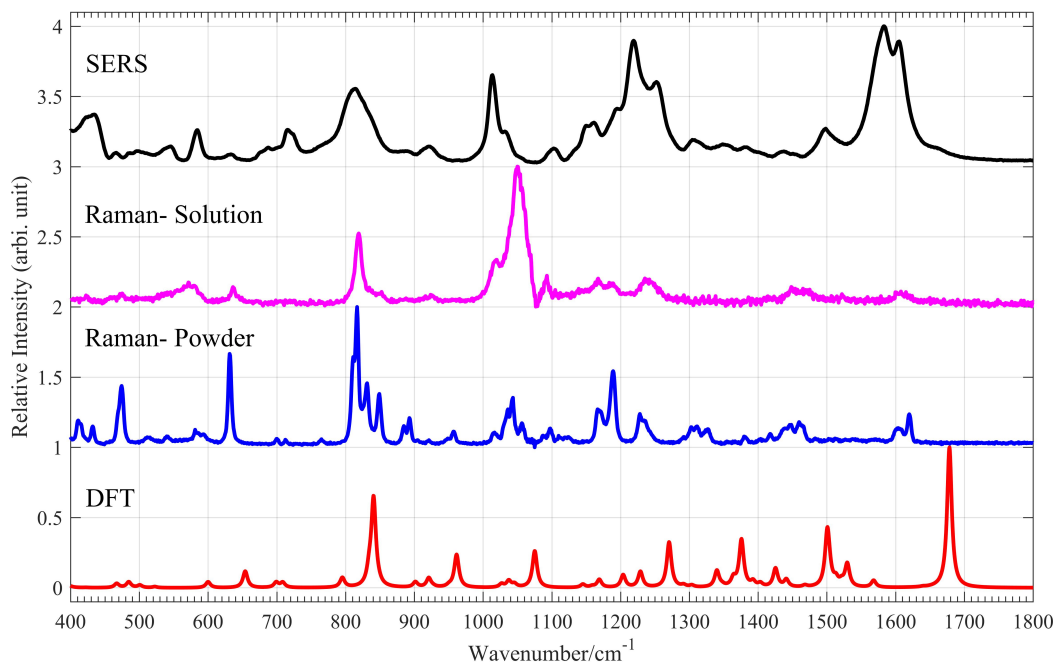


**Figure 30. All pFPP spectra**

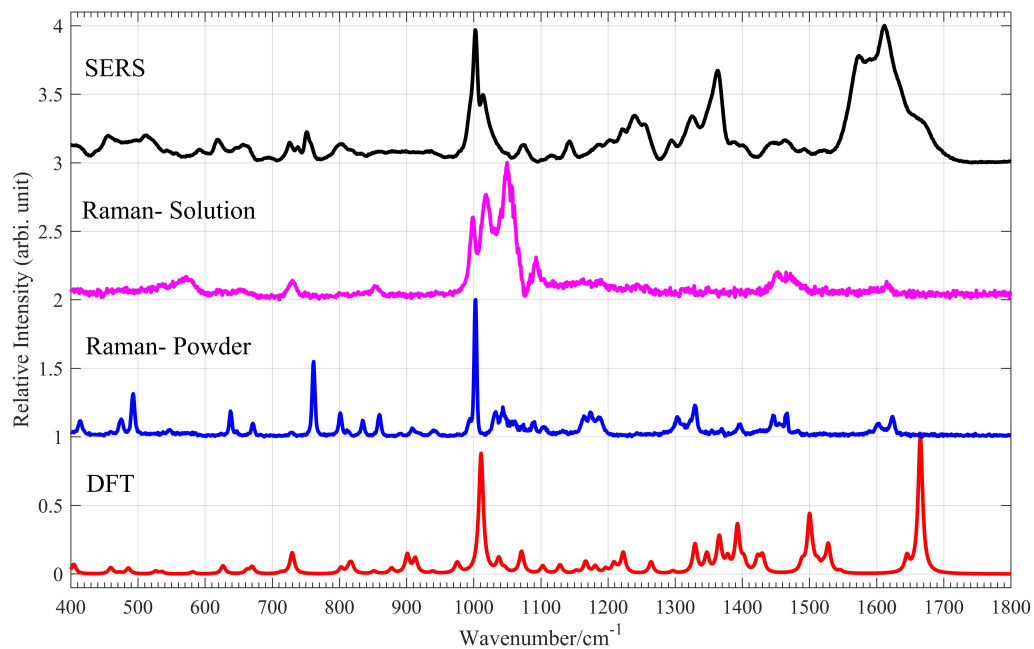


**Figure 31. All TFMP spectra**

**Table 7. Band Assignments for FBZP.**

<b>SERS</b>	<b>Raman-Solution</b>	<b>Raman-Powder</b>	<b>DFT</b>	<b>Description*</b>
446		450	475	$\delta(\text{CNC})_A, \delta(\text{C}=\text{C}-\text{C})_C$
829	828	829	826	$\gamma(\text{CH})_C, \delta_r(\text{CH}_2)_A$
853	859	858	867	$\nu_b(\text{C}=\text{C}-\text{C})_C, \delta_r(\text{CH}_2)_A, \nu(\text{CF})_C$
1020	1018	1041	1007	$\nu(\text{CC})_A, \nu(\text{CN})_A, \delta(\text{CNC})_A$
1159	1168	1167	1227	$\nu(\text{CC})_B, \delta_w(\text{CH}_2)_B, \delta(\text{CH})_C, \delta_t(\text{CH}_2)_A$
1220	1216	1223	1283	$\delta_t(\text{CH}_2)_A, \delta_t(\text{CH}_2)_B$
1265		1253	1323	$\delta(\text{CH})_C, \delta_t(\text{CH}_2)_A, \delta_w(\text{CH}_2)_B$
1452	1453	1448	1436	$\delta_w(\text{CH}_2)_A, \delta_w(\text{CH}_2)_B, \delta(\text{CNC}), \delta(\text{CH})_C$
1596	1607	1602	1520	$\delta_s(\text{CH}_2)_A, \delta(\text{NH})_A$

\*  $\nu$ , stretching;  $\nu_a$ , asymmetric stretching;  $\nu_s$ , symmetric stretching;  $\nu_b$ , ring breathing;  $\delta$ , bending;  $\gamma$ , out-of-plane bending,  $\delta_s$ , scissoring;  $\delta_w$ , wagging;  $\delta_t$ , twisting;  $\delta_r$ , rocking; A, piperazine ring; B, between rings; C, benzene ring

**Table 8. Band assignments for mCPP.**

<b>SERS</b>	<b>Raman-Solution</b>	<b>Raman-Powder</b>	<b>DFT</b>	<b>Description</b>
<b>445</b>			446	$\gamma(\text{C}=\text{C}-\text{C})_C$
<b>683</b>	683	678	690	$\gamma(\text{C}=\text{C}-\text{C})_C, \delta(\text{CCl})_C, \delta_r(\text{CH}_2)_A$
<b>808</b>			820	$\gamma(\text{NH}), \nu_s(\text{CNC})_A$
<b>997</b>	994	988	971	$\nu_b(\text{C}=\text{C}-\text{C})_C, \nu_s(\text{CNC})_A, \delta(\text{CCl})_C$
<b>1014</b>	1018		1006	$\delta(\text{C}=\text{C}-\text{C})_C, \nu(\text{CCl})_C$
<b>1220</b>			1221	$\delta_t(\text{CH}_2)_A, \delta(\text{NH})_A$
<b>1248</b>	1246	1259	1267	$\nu(\text{CN})_B, \delta_t(\text{CH}_2)_A, \delta(\text{CH})_C$
<b>1575</b>			1619	$\nu_a(\text{C}=\text{C}-\text{C})_C, \delta(\text{CH})_C, \delta(\text{CCl})_C$
<b>1607</b>	1597	1595	1654	$\nu_a(\text{C}=\text{C}-\text{C})_C, \delta(\text{CH})_C, \delta(\text{CCl})_C$

**Table 9. Band Assignments for MBZP**

<b>SERS</b>	<b>Raman-Solution</b>	<b>Raman-Powder</b>	<b>DFT</b>	<b>Description*</b>
779	753	749	787	$\nu(\text{CN})_A, \delta(\text{CNC})_A$
812	785	787	829	$\nu(\text{CC})_B, \delta(\text{C}=\text{C}-\text{C})_C, \delta(\text{CN})_B$
851	826	825	867	$\gamma(\text{CH})_C$
996	1005	1001	1020	$\nu_s(\text{C}=\text{C}-\text{C})_C, \delta_r(\text{CH}_2)_B,$
1024	1018	1031	1058	$\nu_s(\text{C}=\text{C}-\text{C})_C, \delta(\text{CH})_C$
1184		1182	1188	$\delta(\text{CNC})_A, \delta_t(\text{CH}_2)_A, \delta_t(\text{CH}_2)_B$
1214	1217	1214	1227	$\nu(\text{CC})_B, \delta(\text{CH})_C, \delta_t(\text{CH}_2), \delta(\text{CH})_C$
1262		1245	1296	$\delta_t(\text{CH}_2)_B, \delta_t(\text{CH}_2)_C, \delta(\text{CH})_C$
1469	1467	1467	1480	$\delta(\text{CH}_3)_A, \delta_s(\text{CH}_2)_A$
1578		1585	1645	$\nu_a(\text{C}=\text{C}-\text{C})_C, \delta(\text{CH})_C, \delta(\text{CC})_B$
1625	1611	1606	1666	$\nu_a(\text{C}=\text{C}-\text{C})_C, \delta(\text{CH})_C, \delta(\text{CC})_B$

**Table 10. Band Assignments for MeOPP**

<b>SERS</b>	<b>Raman-Solution</b>	<b>Raman-Powder</b>	<b>DFT</b>	<b>Description</b>
418			412	$\gamma(\text{CN})_B, \gamma(\text{CO})_C, \delta(\text{CNC})_A$
807	801	807	811	$\gamma(\text{CH})_C, \delta(\text{C}=\text{C}-\text{C})_C$
912			959	$\nu_b(\text{C}=\text{C}-\text{C})_C, \gamma(\text{NH})_A, \nu(\text{CN})_A$
1015	1016	1013	1040	$\nu(\text{CC})_A, \nu_s(\text{CNC})_A$
1178	1187	1185	1218	$\delta(\text{OCH}_3)_C, \delta_t(\text{CH}_2)_A$
1219			1257	$\nu(\text{CN})_B, \delta_t(\text{CH}_2)_A, \delta(\text{CH})_C$
1257	1245	1250	1300	$\nu(\text{COC})_C, \delta(\text{CH})_C, \nu_s(\text{C}=\text{C}-\text{C})_C, \delta_t(\text{CH}_2)_A$
1304			1376	$\delta_w(\text{CH}_2)_A, \nu(\text{CN})_B$
1331		1326	1395	$\delta_r(\text{CH}_2)_A, \delta(\text{NH})_A$
1586	1617	1604	1678	$\nu_a(\text{C}=\text{C}-\text{C})_C, \nu(\text{CO})_C, \delta(\text{CH})_C, \delta(\text{CH}_3)_C$

**Table 11. Band Assignments for pFPP**

<b>SERS</b>	<b>Raman-Solution</b>	<b>Raman-Powder</b>	<b>DFT</b>	<b>Description*</b>
<b>438</b>		432	485	$\delta_r(\text{CH}_2)_A, \delta(\text{CN})_A$
<b>715</b>			709	$\gamma(\text{NH})_C, \delta_r(\text{CH}_2)_A, \delta(\text{CN})_B, \delta(\text{C}=\text{C}-\text{C})_C$
<b>815</b>	819	816	841	$\nu_b(\text{C}=\text{C}-\text{C})_C, \nu(\text{CF})_C, \gamma(\text{NH})$
<b>1013</b>	1050	1043	1075	$\nu_b(\text{C}=\text{C}-\text{C})_C, \nu(\text{CC})_A, \delta(\text{CNC})_A, \nu_s(\text{CNC})_A$
<b>1163</b>	1167	1170	1169	$\delta_r(\text{CH}_2)_A, \nu(\text{CN})_B$
<b>1219</b>	1235	1228	1271	$\nu(\text{CN})_B, \nu_b(\text{C}=\text{C}-\text{C})_C, \delta_t(\text{CH}_2)_A, \nu(\text{CF})_C$
<b>1255</b>			1292	$\nu(\text{CF})_C, \delta(\text{CH})_C$
<b>1496</b>			1501	$\delta(\text{NH})_A, \delta_s(\text{CH}_2)_A$
<b>1579</b>		1600	1640	$\nu_a(\text{C}=\text{C}-\text{C})_C, \delta(\text{CH})_C, \delta(\text{CF})_C$
<b>1606</b>	1607	1620	1678	$\nu_a(\text{C}=\text{C}-\text{C})_C, \delta(\text{CH})_C, \nu(\text{CF})_C$

**Table 12. Band Assignments for TFMPP**

<b>SERS</b>	<b>Raman-Solution</b>	<b>Raman-Powder</b>	<b>DFT</b>	<b>Description*</b>
<b>752</b>	729	761	730	$\delta(\text{CF}_3)_C, \delta(\text{C}=\text{C}-\text{C})_C, \nu(\text{CN})_B$
<b>1002</b>	998	1003	1011	$\nu_s(\text{C}=\text{C}-\text{C})_C$
<b>1015</b>	1017		1037	$\nu(\text{CC})_A, \nu_s(\text{CNC})_A, \delta_w(\text{CH}_2)_A$
<b>1239</b>			1223	$\delta_t(\text{CH}_2)_A, \delta(\text{CH})_C, \delta(\text{NH})_A$
<b>1257</b>			1264	$\nu(\text{CN})_B, \delta(\text{CH})_C, \delta_t(\text{CH}_2)_A$
<b>1324</b>		1330	1366	$\delta_t(\text{CH}_2)_A, \delta_w(\text{CH}_2)_A, \gamma(\text{NH})_A$
<b>1363</b>			1393	$\nu(\text{CN})_B, \delta_t(\text{CH}_2)_A, \nu(\text{CCF}_3)_C$
<b>1571</b>		1601	1645	$\nu_a(\text{C}=\text{C}-\text{C})_C, \delta(\text{CH})_C, \nu(\text{CCH}_3)_C$
<b>1614</b>	1615	1623	1665	$\nu_a(\text{C}=\text{C}-\text{C})_C, \delta(\text{CH})_C, \delta(\text{CCF}_3)_C$

## LIST OF JOURNAL ABBREVIATIONS

Drug Test Anal	Drug Testing and Analysis
Forensic Sci Int	Forensic Science International
J Anal Chem	Journal of Analytical Chemistry
J Anal Tox	Journal of Analytical Toxicology
J Forensic Sci	Journal of Forensic Science
J Med Tox	Journal of Medical Toxicology
J Phys Chem	Journal of Physical Chemistry
J Raman Spectrosc	Journal of Raman Spectroscopy

## BIBLIOGRAPHY

1. Arbo MD, Bastos ML, Carmo HF. Piperazine compounds as drugs of abuse. *Drug and Alcohol Dependence*. 2012 May 1;122(3):174-85.
2. Elliott S. Current awareness of piperazines: pharmacology and toxicology. *Drug Test Anal*. 2011 Jul-Aug;3(7-8):430-8.
3. de Boer D, Bosman IJ, Hidvegi E, Manzoni C, Benko AA, dos Reys L, et al. Piperazine-like compounds: a new group of designer drugs-of-abuse on the European market. *Forensic Sci Int*. 2001 2001;121:47-56.
4. Rosenbaum CD, Carreiro SP, Babu KM. Here today, gone tomorrow...and back again? A review of herbal marijuana alternatives (K2, Spice), synthetic cathinones (bath salts), kratom, *Salvia divinorum*, methoxetamine, and piperazines. *J Med Toxicol*. 2012 Mar;8(1):15-32.
5. BZP, DCP, FBZP, MBZP, TFMPP, MeOPP, pFPP, mCPP; [cited 2016 November 2]; Available from: <https://www.caymanchem.com/>.
6. NFLIS Year 2008 Annual Report; [cited Nov 10 2016]; Available from: [https://www.deadiversion.usdoj.gov/nflis/2008annual\\_rpt.pdf](https://www.deadiversion.usdoj.gov/nflis/2008annual_rpt.pdf)
7. Emerging 2-C Phenethylamines, Piperazines, and Tryptamines in NFLIS 2006-2011; [cited Nov 15 2016]; Available from: [https://www.nflis.deadiversion.usdoj.gov/DesktopModules/ReportDownloads/Reports/NFLIS\\_SR\\_Emerging\\_II.pdf](https://www.nflis.deadiversion.usdoj.gov/DesktopModules/ReportDownloads/Reports/NFLIS_SR_Emerging_II.pdf).
8. Europol–EMCDDA Active Monitoring Report on a new psychoactive substance: 1-(3-chlorophenyl)piperazine (mCPP). [cited Nov 10 2016]; Available from:

[http://www.emcdda.europa.eu/attachements.cfm/att\\_136859\\_EN\\_Europol-EMCDDA\\_Active\\_Monitoring\\_Report\\_mCPP\\_290307.pdf](http://www.emcdda.europa.eu/attachements.cfm/att_136859_EN_Europol-EMCDDA_Active_Monitoring_Report_mCPP_290307.pdf).

9. Gee P, Richardson SK, Woltersdorf W, Moore G. Toxic effects of BZP-based herbal party pills in humans: a prospective study in Christchurch, New Zealand. *The New Zealand Medical Journal*. 2005;118(1227).
10. Elliott S, Smith C. Investigation of the first deaths in the United Kingdom involving the detection and quantitation of the piperazines BZP and 3-TFMPP. *Journal of Analytical Toxicology*. 2008;32:172-7.
11. Helander A, Backberg M, Hulten P, Al-Saffar Y, Beck O. Detection of new psychoactive substance use among emergency room patients: results from the Swedish STRIDA project. *Forensic Sci Int*. 2014 Oct;243:23-9.
12. Takahashi M, Nagashima M, Suzuki J, Seto T, Yasuda I, Yoshida T. Creation and application of psychoactive designer drugs data library using liquid chromatography with photodiode array spectrophotometry detector and gas chromatography-mass spectrometry. *Talanta*. 2009 Feb 15;77(4):1245-72.
13. Farquharson S, Shende C, Sengupta A, Huang H, Inscore F. Rapid detection and identification of overdose drugs in saliva by surface-enhanced Raman scattering using fused gold colloids. *Pharmaceutics*. 2011 Jul 13;3(3):425-39.
14. Saferstein R, editor. *Forensic Science Handbook Volume III*: Pearson, 2010.
15. Diem M. *Introduction to Modern Vibrational Spectroscopy*. New York, NY: John Wiley and Sons, Inc. , 1993.

16. Ferraro J, Nakamoto K. *Introductory Raman Spectroscopy*: Academic Press, Inc. , 1994.
17. Haynes CL, McFarland AD, Van Duyne RP. Surface-Enhanced Raman Spectroscopy. *Journal of Analytical Chemistry*. 2005;77(17):338A-46A.
18. West MJ, Went MJ. Detection of drugs of abuse by Raman spectroscopy. *Drug Test Anal*. 2011 Sep;3(9):532-8.
19. Kneipp K, Kneipp H, Itzkan I, Dasari R, Feld M. Surface-enhanced Raman scattering and biophysics. *Journal of Physics: Condensed Matter*. 2002;14:R597-R624.
20. Jeanmaire DL, Van Duyne RP. Surface raman spectroelectrochemistry: Part I. Heterocyclic, aromatic, and aliphatic amines adsorbed on the anodized silver electrode. *Journal of Electroanalytical Chemistry*. 1977;84(1):1-20.
21. Cînta Pînzaru S, Pavel I, Leopold N, Kiefer W. Identification and characterization of pharmaceuticals using Raman and surface-enhanced Raman scattering. *Journal of Raman Spectroscopy*. 2004;35(5):338-46.
22. Muehlethaler C, Leona M, Lombardi JR. Review of Surface Enhanced Raman Scattering Applications in Forensic Science. *Anal Chem*. 2016 Jan 05;88(1):152-69.
23. Ali EM, Edwards HG. The detection of flunitrazepam in beverages using portable Raman spectroscopy. *Drug Test Anal*. 2016 Mar 16.
24. Inscore F, Shende C, Sengupta A, Huang H, Farquharson S. Detection of drugs of abuse in saliva by surface-enhanced Raman spectroscopy (SERS). *Applied Spectroscopy*. 2011 Sep;65(9):1004-8.

25. Rana V, Canamares MV, Kubic T, Leona M, Lombardi JR. Surface-enhanced Raman spectroscopy for trace identification of controlled substances: Morphine, codeine, and hydrocodone. *J Forensic Sci.* 2011 Jan;56(1):200-7.
26. Sherril CD. Introduction to Density Functional Theory. Georgia Institute of Technology; [cited Jan 10 2017]; Available from: <http://vergil.chemistry.gatech.edu/notes/DFT-intro.pdf>.
27. Ballabio D, Consonni V. Classification tools in chemistry. Part 1: linear models. PLS-DA. *Analytical Methods.* 2013;5(16):3790-8.
28. Using Cross-Validation. Eigenvector Documentation Wiki; [cited March 8 2017]; Available from: [http://wiki.eigenvector.com/index.php?title=Using\\_Cross-Validation](http://wiki.eigenvector.com/index.php?title=Using_Cross-Validation).
29. Patel IS, Premasiri WR, Moir DT, Ziegler LD. Barcoding bacterial cells: A SERS based methodology for pathogen identification. *J Raman Spectrosc.* 2008 Nov;39(11):1660-72.
30. Premasiri WR, Moir DT, Klempner MS, Krieger N, Jones II G, Ziegler LD. Characterization of the surface enhanced Raman scattering (SERS) of bacteria. *J Phys Chem* 2005;109(1):312-20.
31. Le Ru E, Blackie E, Meyer M, Etchegoin P. Surface enhanced Raman scattering enhancement factors: A comprehensive study. *J Phys Chem.* 2007;111:13794-808.
32. SWGDRUG Recommendations; [cited Feb 20 2017]; Available from: <http://www.swgdrug.org/Documents/SWGDRUG%20Recommendations%20Version%2007-1.pdf>

33. Liu L, Chen D, Ma H, Liang W. Spectral Characteristics of Chemical Enhancement on SERS of Benzene-like Derivatives: Franck–Condon and Herzberg–Teller Contributions. *The Journal of Physical Chemistry C*. 2015;119(49):27609-19.
34. Sullivan L. *Essentials of Biostatistics in Public Health*. 2nd ed. Burlington, MA, 2008.

**CURRICULUM VITAE**

